Applied Mathematics and Computation 391 (2021) 125671

Contents lists available at ScienceDirect

Applied Mathematics and Computation

journal homepage: www.elsevier.com/locate/amc

A computational approach to hedging Credit Valuation Adjustment in a jump-diffusion setting☆

Thomas van der Zwaard[a,b], Lech A. Grzelak[a,b], Cornelis W. Oosterlee[a,c]

[a] Delft Institute of Applied Mathematics, Delft University of Technology, Delft, The Netherlands
[b] Rabobank, Utrecht, The Netherlands
[c] CWI - National Research Institute for Mathematics and Computer Science, Amsterdam, The Netherlands

ARTICLE INFO

Article history:
Received 21 May 2020
Revised 24 August 2020
Accepted 6 September 2020
Available online 3 October 2020

Keywords:
Computational finance
Dynamic hedging
Credit Valuation Adjustment (CVA)
Merton jump-diffusion
Counterparty credit risk (CCR)
xVA hedging

ABSTRACT

This study contributes to understanding Valuation Adjustments (xVA) by focussing on the dynamic hedging of Credit Valuation Adjustment (CVA), corresponding Profit & Loss (*P&L*) and the *P&L* explain. This is done in a Monte Carlo simulation setting, based on a theoretical hedging framework discussed in existing literature. We look at hedging CVA market risk for a portfolio with European options on a stock, first in a Black-Scholes setting, then in a Merton jump-diffusion setting. Furthermore, we analyze the trading business at a bank after including xVAs in pricing. We provide insights into the hedging of derivatives and their xVAs by analyzing and visualizing the cash-flows of a portfolio from a desk structure perspective. The case study shows that not charging CVA at trade inception results in an expected loss. Furthermore, hedging CVA market risk is crucial to end up with a stable trading strategy. In the Black-Scholes setting this can be done using the underlying stock, whereas in the Merton jump-diffusion setting we need to add extra options to the hedge portfolio to properly hedge the jump risk. In addition to the simulation, we derive analytical results that explain our observations from the numerical experiments. Understanding the hedging of CVA helps to deal with xVAs in a practical setting.

1. Introduction

Since the 2007–2008 global financial crisis, financial institutions have been required to apply and report Valuation Adjustments (xVAs) for over-the-counter (OTC) derivatives and hedge the associated risks. These adjustments to the risk-neutral price of a derivative account for previously neglected risks that were revealed during the crisis. Credit Valuation Adjustment (CVA), corresponding to Counterparty Credit Risk (CCR), was the first of many xVAs. CVA volatility is one of the major drivers behind the large losses observed during the crisis [3]. Linear contracts[1] are no longer linear when CCR is included in the valuation. Hence, not including CCR in pricing results in an incorrect hedging policy. Next, xVA pricing evolved with various other xVAs, see [1,2] for more information. Calculating the increasing number of xVAs is computationally challenging, and has attracted significant academic and corporate interest.

☆ The views expressed in this paper are the personal views of the authors and do not necessarily reflect the views or policies of their current or past employers.

E-mail addresses: T.vanderZwaard@tudelft.nl (T. van der Zwaard), L.A.Grzelak@tudelft.nl (L.A. Grzelak), C.W.Oosterlee@cwi.nl (C.W. Oosterlee).

[1] Linear contracts/instruments have contractual cash-flows that are a linear function of the underlying.

https://doi.org/10.1016/j.amc.2020.125671
0096-3003/

The first literature on xVA pricing appeared before and during the crisis [4–6]. To date, several books have addressed the topic [1,2,7]. There are three streams in literature on xVA pricing, all describing the mathematical problem in different ways. First of all, there approach where the xVA is expressed as an expectation, which can numerically be approximated using a Monte Carlo approach. A set of risk factors is simulated in a Monte Carlo engine, after which the future exposures that contribute to the xVA metrics are evaluated along the simulated paths [8–12]. The Monte Carlo approach allows for scalable computations. Hence, this type of method is typically implemented by banks. Second, there is the PDE approach that aims to solve the xVA PDE directly [13,14]. Dimensionality is one of the downsides of this approach, though low-dimensional non-linear problems can be treated highly accurately. Last, there is the BSDE approach, which may be non-trivial in a regression based Monte Carlo approach [15–19]. Literature on xVA has focussed on deriving the mathematical pricing equations, as well as addressing the computational challenges that arise when solving these pricing equations. In our work, we closely examine xVA pricing and market risk hedging. We focus on the dynamic hedging of CVA market risk, where we study the cash-flows of a portfolio from a desk structure perspective. This results in an improved understanding of the CVA hedging mechanics. We show that the CVA market risk in the portfolio needs to be hedged to end up with a stable trading strategy.

The trading strategy is a combination of all trading positions with a counterparty and the corresponding hedging strategy [11,12]. A wealth account [20] is connected to this trading strategy, it tracks the total wealth of the trading strategy over time. This is a cash account that accrues interest. Bielecki and Rutkowski formalized this framework [15]. The generic trading strategy formulation provides a useful framework to analyze exchanges of assets and cash. Furthermore, the generic formulation is useful for the hedging of xVAs. We provide numerical examples and insights in a Monte Carlo simulation setting, starting in the Black-Scholes world.

The constant volatility is one of the known shortcomings of the Black-Scholes model. The resulting flat implied volatility is in clear contrast with the market's implied volatility smile. To properly manage this smile risk, several streams of modelling have emerged. Among these approaches are the local volatility models (e.g., Dupire [21], Derman and Kani [22]) and the stochastic (local) volatility models (e.g., Heston [23], Hagan *et al.* [24], Lipton [25]). Although these models fit in the generic hedging framework, we choose to focus on jump-diffusion models, which exhibit heavy tails in the distribution of stock returns and fit well with the jump patterns observed for stocks. Jump-diffusion models extend the Black-Scholes model with independently distributed jumps driven by a Poisson process. Typical choices of jump size distributions are a double exponential distribution, Kou [26], or normal distributed jumps, Merton [27]. We choose to work with the latter. Further research on the Merton jump-diffusion model has been on calibrating the model and hedging the jump risk that partially drives option prices under this model [28,29].

Therefore, after studying the dynamic hedging of CVA market risk in a Black-Scholes setting, we do the same in a Merton jump-diffusion setting. In addition, we examine the impact of defaults on the portfolio. The Profit and Loss of the trading strategy is examined to assess the hedge's performance. We show that, for a portfolio of European options, not including CVA in the pricing results in an expected loss. Hence, we interpret CVA as a fair compensation for the credit risk of the counterparty. Charging CVA to the client at trade inception overcomes the expected loss. CVA can be treated as a cash amount, however, this ignores the dependencies of the CVA on the market variables. After including the CVA hedge in the strategy, we assess the impact of jumps in the underlying stock on the portfolio. In particular, we find that in the context of CVA, the jump risk can be mitigated to a large degree by adding extra hedging instruments to the strategy. Rather than merely performing a simulation, we also derive analytic results to understand and explain our numerical observations.

This paper is organized as follows. In Section 2 we provide background information on Profit and Loss, which is used to examine the outcome of the hedging strategies. In Section 3 we introduce the trading strategy and the corresponding wealth account. Next, the numerical simulation of the future market states and results of the various hedging strategies will be addressed in Sections 4 and 5 respectively. Finally, the work is concluded in Section 6.

2. Profit and loss

Profit and Loss (*P&L*) is a financial institution's income statement. This is an officially reported number that summarizes the change in *Mark-to-Market* (MtM) value over a period of time, normally one business day. During this period, the institution examines which part of the change in MtM can be attributed to market moves and other predefined effects, such as the passing of time. This process is also called *P&L attribution*, or *P&L explain*, which explains the impact of the daily market movements on the value of the portfolio. The goal is to verify that the modelled risk factors satisfactorily explain the change in portfolio value. The *P&L* explain process runs after the closing of every business day, so it is a backward looking measure. Typically, the variance between two consecutive days is also examined.

A financial institution wants to explain the *P&L* as well as possible. Hence the residual *P&L*, which from now on we address as *P&L unexplained*, should be as small as possible. Yet explaining all *P&L* is insufficient, as extreme numbers that are completely explained are also undesirable. Therefore, institutions put thresholds/limits on both *P&L* and *P&L* unexplained at a portfolio level, where the thresholds depend on the portfolio composition. In addition to these *P&L* limits, market risk limits on particular risk types are in place for both traders and portfolios. The aim of these market risk limits is to make sure the trading activities remain within the institution's predefined risk appetite and that exposure to certain market drivers is bounded. This naturally limits the *P&L* as well. The portfolios are not always entirely flat in terms of risk, as in practice it is not feasible to rebalance the hedge daily, for example due to transaction costs. Furthermore, having a flat portfolio is not

always the goal as this may be a way to express a view on the market. In practice, the residual risk of a portfolio is being monitored.

For xVAs a separate explain process exists, which is analogous to the one for the MtM value. Limits on market risk drivers, *P&L* and *P&L* unexplained are present.

In literature the following approaches to *P&L* explain can be found [1,30]:

1. Let $V(t,\ \gamma(t))$ denote value V at time t with a set *market data* $\gamma(t)$. The first approach is a Taylor-based explain process where the partial derivatives of the instrument V with respect to $\gamma(t)$ are used to explain the difference in $V(t_{k-1}, \gamma(t_{k-1}))$ and $V(t_k,\ \gamma(t_k))$, $t_{k-1} < t_k$.[2] In other words,

$$V(t_k, \gamma(t_k)) - V(t_{k-1}, \gamma(t_{k-1})) = \left.\frac{\partial V}{\partial t}\right|_{t_{k-1}} \mathrm{d}t + \mathcal{A}(t_{k-1}) + P\&L_U(t_k),$$
$$\mathcal{A}(t_{k-1}) = \sum_{i=1}^{n} \left.\frac{\partial V}{\partial \gamma_i}\right|_{t_{k-1}} \mathrm{d}\gamma_i + \frac{1}{2}\sum_{i=1}^{n}\sum_{j=1}^{n} \left.\frac{\partial^2 V}{\partial \gamma_i \partial \gamma_j}\right|_{t_{k-1}} \mathrm{d}\gamma_i \mathrm{d}\gamma_j. \tag{2.1}$$

   The left hand side of Eq. (2.1) is $P\&L(t_k)$. $P\&L_U(t_k)$ is the unexplained *P&L*. The remaining terms can be interpreted as $P\&L_E(t_k)$, i.e., the explained *P&L*.
2. In the second approach, the *theta effect* $\left.\frac{\partial V}{\partial t}\right|_{t_{k-1}} \mathrm{d}t$, is neglected and we are only interested in the change of value V in the interval $\left[t_{k-1}, t_k\right]$ as a result of movements in the underlying market data γ_i.[3] In other words,

$$V(t_{k-1}, \gamma(t_k)) - V(t_{k-1}, \gamma(t_{k-1})) = \mathcal{A}(t_{k-1}) + P\&L_U(t_k). \tag{2.2}$$

   The left hand side of Eq. (2.2) is $P\&L(t_k)$, and the $\mathcal{A}(t_{k-1})$ term is $P\&L_E(t_k)$. The effect of ignoring the theta should not be too large, as *P&L* explain is a daily process, but the size of the effect will depend on the portfolio composition. This method considers instrument values at the same date, and the difference in value is caused by a perturbed market data set.
3. Another approach is a high-level attribution using effects to explain the *P&L* in a consecutive manner.[4] Before starting the explain process, a list of effects is composed, which are applied one-by-one. After applying an effect, the portfolio is revalued and the difference is attributed to the particular effect. These changes will be permanent, so when applying a new effect, the old effects stay in place. This implies that cross-effects are introduced, which cannot be allocated properly, as well as an order dependence on the effects. Yet this approach should yield similar results as the previous ones. Examples of the effects used in the *P&L* attribution can be: time decay (including holiday effects, carry effects as well as shifts in market data), market data changes (IR / FX / inflation / bonds / credit), turns, fixings, and trade closing.

When a financial institution observes jumps in *P&L*, these are investigated. Real-world jumps are typically caused by trade insertions or cancellations (captured via the theta term), rather than by underlying market movements. Though theta contributions will be present in practice, they are not relevant for our discussion, which focusses on the effect of market movements on the *P&L* of a portfolio. Hence we use the orthogonal explain approach as per Eq. (2.2), which makes use of perturbed market data. Here we can simply take the next day's market data as the perturbed market data.

3. Hedging framework

We start with a risk-neutral pricing framework, where we consider the various contributions to the price of a derivative. Using the standard replicating portfolio argument [7], the price of a derivative is equivalent to the price of a replicating portfolio containing other securities.

We define a trading strategy as a combination of positions in a set of available trading instruments, accompanied by the hedging positions in hedging instruments, which mitigate the market risk associated with the positions in the trading instruments. We assume that the short-selling of all assets is possible. In practice, hedges do not necessarily mitigate all the market risk, but certain limits are placed per market risk factor on a portfolio level. A trader will make sure that the exposure of a portfolio to certain risk factors will remain below these predefined thresholds by taking the necessary positions in market instruments. Here we will assume that all the market risk is always reduced by the dynamic hedging strategy, i.e., we choose the hedging positions that together replicate the risk profile of the trading positions as good as possible.

[2] Green refers to this as "risk-based explain" [1, Section 21.1.4]. Andersen and Piterbarg use the term "second order *P&L* predict" [30, Section 22.2.1].

[3] Green refers to this as "orthogonal explain" [1, Section 21.1.4]. Andersen and Piterbarg use the term "perturbed market data approach" [30, Section 22.1.5].

[4] Green refers to this as "step-wise explain" [1, Section 21.1.4]. Andersen and Piterbarg use the term "bump and do not reset" type of *P&L* explain, a.k.a. the "waterfall explain" [30, Section 22.2.2.1].

The *trading strategy* $\Pi(t)$ is generically defined for N *trading instruments* $V_i(t)$ in which *trading positions* $\zeta_i(t)$ are taken, which are assumed to be exogenously provided. Analogously, we consider M *hedging instruments* $H_i(t)$ in which *hedging positions* $\eta_i(t)$ are taken. The trading strategy $\Pi(t)$ is then summarized as follows:

$$\Pi(t) = \sum_{i=1}^{N} \zeta_i(t) V_i(t) + \sum_{i=1}^{M} \eta_i(t) H_i(t). \tag{3.1}$$

We start in a Black-Scholes setting, where European options are considered for the sake of clarity and ease of computation. However, the generic formulation allows for much more flexibility, for example, for the case of a large portfolio of interest rate swaps. The underlying interest rate risks are then eliminated by taking hedging positions in the par instruments used to build the underlying yield curve(s) that are in turn required to value the portfolio of interest rate swaps.

Define the *cash-flows* for the trading and hedging instruments respectively by $c^V_{i,j}(t)$ and $c^H_{i,j}(t)$, denoting the time t value of the j-th cash-flow paid at time T_j, corresponding to respectively instruments V_i and H_i, which in total generate respectively n_i and m_i cash-flows. We then define the time t value of the cumulative cash-flows corresponding to instrument V_i and H_i respectively as

$$C^V_i(t) = \sum_{j=1}^{n_i} \zeta_i(T_j) c^V_{i,j}(t) 1_{\{T_j \le t\}}, \quad C^H_i(t) = \sum_{j=1}^{m_i} \eta_i(T_j) c^H_{i,j}(t) 1_{\{T_j \le t\}}, \tag{3.2}$$

which is to be interpreted as the quantity representing all cash-flows paid up and till time t, taking into account the time value of money, $B(t)$, being the *bank account*. This is the solution of $\mathrm{d}B(t) = r(t)B(t)\mathrm{d}t$, where $B(t_0) = 1$ and with *risk-free rate* $r(t)$.

In parallel with the trading strategy $\Pi(t)$, we define a *wealth process* $w(t)$ that represents the total wealth realized over time, obtained by summing up all the profits and losses over time. There are two sources for changes in wealth: one is the rebalancing of positions in instruments, the other results from cash-flows associated with the various instruments. We assume that $V_i(t)$ and $H_i(t)$ denote the value after exchange of all cash-flows at time t. For example, if a cash-flow takes place at date t, the values $V_i(t)$ and $H_i(t)$ do not contain the value of this cash-flow. Rebalancing the trading positions, and consecutively the hedging positions, takes place after the exchange of cash-flows. The wealth is a cash amount that accrues interest over time at the risk-free rate, which means that we assume the institution can borrow and lend at the risk-free rate.

At time t_0, the wealth will be composed of the cost to enter the positions in all instruments, including any potential cash-flows taking place at t_0:

$$w(t_0) = -\Pi(t_0) + \sum_{i=1}^{N} C^V_i(t_0) + \sum_{i=1}^{M} C^H_i(t_0). \tag{3.3}$$

The rebalancing of the trading and hedging positions is denoted by $\mathrm{d}\zeta_i(t)$ and $\mathrm{d}\eta_i(t)$ respectively. We write the following (recursive) expression for the wealth at $t_0 \le t_{k-1} < t_k$:

$$\begin{aligned} w(t_k) = w(t_{k-1}) \frac{B(t_k)}{B(t_{k-1})} &- \sum_{i=1}^{N} B(t_k) \int_{t_{k-1}}^{t_k} \frac{V_i(u)}{B(u)} \mathrm{d}\zeta_i(u) + \sum_{i=1}^{N} B(t_k) \int_{t_{k-1}}^{t_k} \frac{\mathrm{d}C^V_i(u)}{B(u)} \\ &- \sum_{i=1}^{M} B(t_k) \int_{t_{k-1}}^{t_k} \frac{H_i(u)}{B(u)} \mathrm{d}\eta_i(u) + \sum_{i=1}^{M} B(t_k) \int_{t_{k-1}}^{t_k} \frac{\mathrm{d}C^H_i(u)}{B(u)}. \end{aligned} \tag{3.4}$$

The first term in Eq. (3.4) is the wealth at the previous point in time t_{k-1} that has accrued interest. This is followed by the re-balancing and cash-flows of respectively the trading and hedging instruments.

The continuous time formulation from Eq. (3.4) is discretized in time $t_0 < t_1 < \ldots < t_{k-1} < t_k \ldots < t_K$: [5]:

$$w(t_k) \approx w(t_{k-1}) \frac{B(t_k)}{B(t_{k-1})} - \sum_{i=1}^{N} V_i(t_k) \mathrm{d}\zeta_i(t_k) + \sum_{i=1}^{N} \mathrm{d}C^V_i(t_k) - \sum_{i=1}^{M} H_i(t_k) \mathrm{d}\eta_i(t_k) + \sum_{i=1}^{M} \mathrm{d}C^H_i(t_k). \tag{3.5}$$

In this context, the initial wealth from Eq. (3.3) remains valid. Furthermore, t_K is the final time at which either all trading instruments have matured, or at which all positions are closed. We keep the positions in trading and hedging instruments constant over a time interval $(t_{k-1}, t_k]$. The terms $\mathrm{d}C^V_i(t_k)$ and $\mathrm{d}C^H_i(t_k)$ respectively represent the trading and hedging instruments' cash-flows present in time interval $(t_{k-1}, t_k]$:

$$\mathrm{d}C^V_i(t_k) = \sum_{j=1}^{n_i} \zeta_i(T_j) c^V_{i,j}(t_k) 1_{\{t_{k-1} < T_j \le t_k\}}, \quad \mathrm{d}C^H_i(t_k) = \sum_{j=1}^{n_i} \eta_i(T_j) c^H_{i,j}(t_k) 1_{\{t_{k-1} < T_j \le t_k\}}. \tag{3.6}$$

[5] For a generic function $f(\cdot)$ we define $\mathrm{d}f(t_k) = f(t_k) - f(t_{k-1})$.

Strategy (3.1) is by design *self-financing*, i.e., there is no cash in- and/or outflow during the lifetime of the strategy. In other words, $\Pi(t) + w(t) = 0$ holds on average. At t_0 we assume that any funding required to set up the trading strategy is obtained from the internal Treasury department.

3.1. Output metrics

Now that the trading strategy $\Pi(t)$ and wealth $w(t)$ are defined, we define several output metrics to evaluate the performance of the trading strategy. In a perfect world, the self-financing constraint $\Pi(t) + w(t) = 0$ holds on average for all $t_k \in [t_0, t_K]$, i.e.,

$\mathbb{E}_{t_0}[\Pi(t_k) + w(t_k)] = 0$. In particular, we are interested in this condition at final time t_K, where all open positions are closed such that $\Pi(t_K) = 0$. So, we evaluate the *expected terminal wealth*: $\mathbb{E}_{t_K}[w(t_0)]$. Assuming that one can continuously rebalance the hedging positions, the terminal wealth should be zero on average.

In addition to the terminal wealth, we also examine *P&L*. The relevant market information at time t is represented by $\gamma(t)$ and we rewrite $V_i(t)$ as follows: $V_i(t) = V_i(t, \gamma(t))$. This allows us to price product V_i at time t with a set of market data $\gamma(t)$. In a similar fashion, we write $H_i(t) = H_i(t, \gamma(t))$. Define the following *P&L* quantities corresponding to trading strategy (3.1):

$$P\&L_V(t_k) = \sum_{i=1}^{N} \zeta_i(t_{k-1})[V_i(t_{k-1}, \gamma(t_k)) - V_i(t_{k-1}, \gamma(t_{k-1}))], \tag{3.7}$$

$$P\&L_H(t_k) = \sum_{i=1}^{M} \eta_i(t_{k-1})[H_i(t_{k-1}, \gamma(t_k)) - H_i(t_{k-1}, \gamma(t_{k-1}))], \tag{3.8}$$

$$P\&L_P(t_k) = P\&L_V(t_k) + P\&L_H(t_k). \tag{3.9}$$

$P\&L_V$ in Eq. (3.7) is the *P&L* generated by the trading positions. When the hedging quantities $\eta(t)$ are based on sensitivities of the trading positions, $P\&L_H$ in Eq. (3.8) can be seen as a first-order *P&L* explain. By choosing the same instruments for hedging as for the daily *P&L* explaining process, we are in fact looking at how well the hedging strategy is able to explain changes in value of the trading strategy as a result of changes in the market data.

The residual risk, after combining trading and hedging positions, is represented by $P\&L_P$ in Eq. (3.9). As the hedge is constructed to eliminate all desired sources of randomness, the daily change portfolio value is automatically equal to the $P\&L_P$, i.e., we can rewrite $P\&L_P$ from Eq. (3.9) by means of Eqs. (3.7) and (3.8):

$$P\&L_P(t_k) = \Pi(t_{k-1}, \gamma(t_k)) - \Pi(t_{k-1}, \gamma(t_{k-1})). \tag{3.10}$$

We then use the orthogonal *P&L* attribution process from Eq. (2.2) to assess which portion of the residual risk can be explained. Note the absence of cash-flows in this discussion. This is because we want to treat cash-flows in a consistent manner, such that only the market movements are attempted to be explained.

4. Market simulation

The hedging framework from Section 3 will be used in a numerical simulation setting to assess Valuation Adjustments and the hedging thereof. The starting point of the numerical analysis is choosing a portfolio of trading instruments and the corresponding hedging instruments. The economic value of a trading instrument is the combination of the risk-free value and Valuation Adjustments, where we choose to look at CVA only. We consider only European options for the trading instruments. DVA turns out to be trivial for this portfolio composition, so DVA is ignored in the analysis. CVA computations require the following two main components: market exposure and default probability. The former is introduced in Section 4.1, the latter is discussed here directly.

We model the jump-to-default by a Poisson process $X_{\mathcal{P}}(t)$ with constant hazard rate $\lambda(t) = \xi_{\mathcal{P}}$, i.e. a homogenous Poisson process. [6] The deterministic hazard rate (e.g., constant or piece-wise constant) implies that credit events [7] are independent of the interest rates and deterministic recovery rates. In addition, assume that the *recovery rate R* is deterministic. *Survival probability SP(t, T)* is the probability that the counterparty will survive until time *T*, conditional on survival till time *t*:

$$SP(t,T) = \mathbb{E}_t\left[\exp\left\{-\int_t^T \lambda(s)\mathrm{d}s\right\}\right] = \exp\left\{-\int_t^T \lambda(s)\mathrm{d}s\right\} = \mathrm{e}^{-\xi_{\mathcal{P}}(T-t)}.$$

A credit curve is the credit-analogue of the yield curve, where we do not extract discount factors but survival probabilities from the curve. In a market implied setting, survival probabilities $SP(t_0, T)$ are extracted from the market using quotes of

[6] To gain some intuition on how this Poisson processes works, look at its expected value $\mathbb{E}[X_{\mathcal{P}}(t)] = \xi_{\mathcal{P}} t$, which is the expected number of events in a time interval with length *t*. So say we have an interval $[0, T]$ of length T where we expect one event every $2T$, then we must set $\xi_{\mathcal{P}} = \frac{1}{2T}$.

[7] A credit event is considered to be the first event of a Poisson counting process which occurs at some random time τ with probability $\mathbb{P}(X_{\mathcal{P}}(\tau + \mathrm{d}t) - X_{\mathcal{P}}(\tau) | X_{\mathcal{P}}(\tau) = 0)$, i.e., the probability of default in interval $[\tau, \tau + \mathrm{d}t)$ conditional on survival until time τ.

highly standardized CDSs. For CVA calculations we require knowledge about the *probability of default* PD(*t, T*) of a counterparty in a certain time interval [*t, T*]. The probability of default is related to the survival probability: $\text{PD}(t,T) = 1 - SP(t,T)$.

We choose to hedge all the market risk introduced by the risk-free value and CVA corresponding to the trading instruments. We do not consider the credit risk component introduced by the CVA. This means that jump risk upon default is not hedged dynamically, meaning that credit risk warehousing takes place. CDS positions can be used to hedge this residual risk [1,2], which fits within the current framework. In Section 4.2 we look in more detail at the setup of the trading strategy.

4.1. Model-free european option exposures

Given a call option V that runs from t_0 till maturity t_K, we create a grid of *monitoring dates* $t_0 < t_1 < \ldots < t_k \ldots < t_K$ at which we compute *exposures*. The following convenient result can easily be derived for the *discounted expected positive exposure* (EPE) of a call/put option:

$$\text{EPE}(t_0, t_k) = V(t_0). \tag{4.1}$$

Using the result from Eq. (4.1) in the formula for CVA, assuming no *Wrong Way Risk (WWR)*, yields:

$$\begin{aligned}\text{CVA}(t_0) &= (1-R)\sum_{k=1}^{K}\text{EPE}(t_0,t_k)\text{PD}(t_{k-1},t_k)\\ &= (1-R)\sum_{k=1}^{K}V(t_0)\text{PD}(t_{k-1},t_k)\\ &= (1-R)V(t_0)\text{PD}(t_0,t_K).\end{aligned} \tag{4.2}$$

The results in Eqs. (4.1) and (4.2) are model-free up to the level how $V(t)$ is computed. [8]

4.2. Simulation framework

For our trading instruments we choose a constant long unit position (i.e., buy) in a European call option $V_1(t)$, i.e., $N = 1$ and $\zeta_1(t) = 1\ \forall t$. [9] The option is assumed to be an OTC deal where the underlying asset $S(t)$ is a third-party asset, i.e., $S(t)$ is not the asset of the option seller. This implies the absence of WWR, meaning we assume that the creditworthiness of the option seller and buyer and the underlying asset move independently. In addition, we assume a constant credit curve over time, i.e., no stochasticity for the credit is used. Furthermore, we assume the option has a cash-settled payoff. The market risk of the option is hedged by buying/selling the underlying stock from/to an exchange, i.e., $M = 1$ and $H_1(t) = S(t)$:

$$\Pi(t) = V_1(t) + \eta_1(t)S(t), \tag{4.3}$$

where $\eta_1(t)$ depends on a model chosen by the financial institution. Hedging positions $\eta_1(t)$ are rebalanced on a daily basis. We assume no dividends are paid, though they can easily be added to the framework in the form of cash-flows. The trading instrument will generate one cash-flow, namely the payoff at maturity in case the option is in the money and the counterparty has not defaulted.

The trading instruments $V_i(t)$ can represent the risk-neutral value, which corresponds to the case without Counterparty Credit Risk (CCR). On the other hand, it can also represent the economic value, which is the sum of the risk-neutral value and xVAs that are taken into account, and corresponds to the case where CCR is taken into account, i.e.,

$$\begin{cases} V_1(t) &:= V(t), & \text{(the case without CCR)}\\ V_1(t) &:= V(t) - \text{CVA}(t) & \text{(the case with CCR)}\\ &\ = V(t)(1-(1-R)\text{PD}(t,t_K)), & \end{cases} \tag{4.4}$$

where for the case with CCR we used Eq. (4.2). Recall that $V(t)$ represents the risk-free value of the option, whereas $V_1(t)$ represents the risky value of the option. This composition of two terms also needs to be taken into account when determining hedging position $\eta_1(t)$: do we hedge only $V(t)$ or also $\text{CVA}(t)$?

First, the market ($S(t)$, $V_i(t)$ and $H_i(t)$) is simulated using a model (e.g., Black-Scholes or Merton jump-diffusion). While valuing the portfolio, these numbers are assumed to be exogenous, meaning there is no longer a model dependence. The model used to compute the hedging quantities and perform the *P&L* explain needs to be calibrated to the market. When this model is the same as the model used to simulate the market, the calibration is trivial.

We use two strategies, Π^{NoCCR} and Π^{CCR}, to assess the effect of CCR. The former corresponds to the portfolio without simulation of defaults, while the latter includes CCR by simulating default times. In all cases, the hedges are rebalanced daily and assumed to be free of CCR. The simulated *default times* $\tau = t_d$ are drawn from the same distribution that drives

[8] CVA is in essence a compound option on the value of a portfolio. A compound option refers to an option on an option. Say that we consider a portfolio of a single option, then the max function in the expected exposure in the CVA formula makes the CVA a compound option.

[9] This reverse Black-Scholes hedge is an academic setup, as buying a call option and hedging the delta risk is not what one usually encounters. However, for illustrative purposes this particular setting is chosen.

the credit curve. So, the simulated default times are the first jumps of $X_{\mathcal{P}}(t)$. In the experiments, we assume a *risk-free closeout*, where we give back V_1 to the defaulted counterparty, and in return receive $R \cdot V(\tau)$ in case this value is positive. We assume stock $S(t)$ to be independent of any default events of the counterparty. At default, we re-enter the same deal, at zero additional costs, with another counterparty which is assumed to be credit risk free, for example a clearing house. This approach is in line with considering the CVA as the cost of hedging counterparty credit risk, regardless of a counterparty default. If the CVA market risk is hedged, this hedge position is closed at default.

4.3. Black-Scholes dynamics

So far we have not assumed any model for $S(t)$ and $V_1(t)$, only a choice of credit curve and simulation of defaults was made. The next step is to assume a model for $S(t)$ and $V_1(t)$. Our first choice is the Black-Scholes model that allows for analytical option prices and derivatives, in a deterministic interest rate setting. Recall the Black-Scholes SDE under real-world measure $\mathbb{P}$:

$$\mathrm{d}S(t) = \mu S(t)\mathrm{d}t + \sigma S(t)\mathrm{d}W^{\mathbb{P}}(t). \tag{4.5}$$

For the simulation of the market scenarios, the SDE (4.5) is discretized using an Euler scheme. The risk introduced by the underlying stock is eliminated when choosing the Black-Scholes delta hedging quantity:

$$\eta_1(t) = -\frac{\partial V_1(t)}{\partial S}. \tag{4.6}$$

In the risk-free case where $V_1(t) = V(t)$, hedging quantity (4.6) holds directly. [10] On the other hand, in the risky case $V_1(t) = V(t) - \mathrm{CVA}(t)$, where CVA is hedged, we can write the following using result (4.2):

$$\eta_1(t) = -\frac{\partial V(t)}{\partial S}(1 - (1-R)\mathrm{PD}(t, t_K)). \tag{4.7}$$

In our experiments, we simulate the synthetic market and do all pricing under the $\mathbb{Q}$ dynamics. Indeed, the stock dynamics in Eq. (4.5) are under the $\mathbb{P}$ measure. Under this measure, delta neutrality is imposed and the hedging quantities are derived. The pricing of the derivatives and calculating risks as in Eqs. (4.6) and (4.7) is then done under $\mathbb{Q}$ (after imposing a no-arbitrage argument), which is in line with risk-neutral pricing theory. Then, a synthetic market is created by means of a real-world evolution under the $\mathbb{P}$ measure with drift μ. In particular, in our numerical experiments we choose the two measures to collapse to the same through the choice of μ and using the risk-neutral Brownian motion. For the simulated defaults we assume $\mathbb{Q}$ defaults, which can for example be obtained through a calibration of the chosen credit model to CDSs. Alternatively, one could plug in historic $\mathbb{P}$ data and still do the valuation and risk calculation under $\mathbb{Q}$.

The simulation is illustrated by a series of schematic drawings that indicate the flow of cash and instruments, see Appendix C. There we consider both the internal exchange of cash-flows and products between the trading desk and xVA desk, as well as the external exchange with the counterparty and other market entities.

4.4. Merton jump-diffusion dynamics

Jump-diffusion models aim to overcome the Black-Scholes assumption of constant implied volatility, by introducing independently distributed jumps in the dynamics. They can generically be defined as [7]:

$$\mathrm{d}X(t) = \mu\mathrm{d}t + \sigma\mathrm{d}W^{\mathbb{P}}(t) + J(t)\mathrm{d}X_J^{\mathbb{P}}(t), \quad S(t) = \mathrm{e}^{X(t)}. \tag{4.8}$$

The *jumps* J arrive according to *Poisson process* $X_J^{\mathbb{P}}(t)$ that is assumed to be independent of the Brownian process $W^{\mathbb{P}}(t)$. Typical choices of jump size J distributions are a double exponential distribution as introduced by Kou [26] or normally distributed jumps as introduced by Merton [27]. We choose to work with the latter. Jump magnitudes in this model follow distribution $J \sim \mathcal{N}\left(\mu_J, \sigma_J^2\right)$.

For the simulation of a synthetic market we use an Euler discretization of the $\mathbb{P}$ dynamics from Eq. (4.8). On the other hand, for pricing options and calculating risks we need $\mathbb{Q}$ dynamics. To obtain these, in Eq. (4.8) we should choose the drift as follows [11]:

$$\mu = r - \xi_J \mathbb{E}\left[e^J - 1\right] - \frac{1}{2}\sigma^2 = r - \xi_J\left(\mathrm{e}^{\mu_J + \frac{1}{2}\sigma_J^2} - 1\right) - \frac{1}{2}\sigma^2.$$

Furthermore, we use a risk-neutral Brownian motion and jump process in the $\mathbb{Q}$ dynamics, which are again assumed to be independent. For European option prices under the Merton jump-diffusion model an analytic expression exists, see A.1.

After simulating the market $S(t) = \mathrm{e}^{X(t)}$ with the Merton model, we compute the Merton option price using Eq. (A.1). Here we do not make an assumption on $V_1(t)$ being a risk-free or risky option value (without CVA versus with CVA). Distinguishing between the two cases can be done in a similar fashion as discussed in Section 4.3.

[10] We do not go into the way the delta hedge is set up, for example via the repo market, as we do not consider funding effects in this paper.

[11] In this case we can use the known result that for $A \sim \mathcal{N}\left(\mu, \sigma^2\right)$ we know $\mathbb{E}\left[e^A\right] = \mathrm{e}^{\mu + \frac{1}{2}\sigma^2}$.

To choose an appropriate hedging strategy, we have another look at the trading instrument we are trying to hedge, including the way the value is determined. The option pricing formula (A.1) contains an infinite sum of scaled Black-Scholes option prices, which is a direct result of the jump size following a continuous distribution. Thus, in an attempt to hedge the jump risk introduced by the model, one would theoretically need infinitely many options, which is practically infeasible. Hedging the jump risk has been addressed by adding a number of options to the hedging portfolio [28,29]. This significantly reduces the variance of the portfolio. In particular, a local minimal variance hedging strategy was examined, combined with a delta position in the underlying stock. In this paper, we use the analytical jump parameter sensitivities from A.1 to determine the hedging positions that aim to eliminate the underlying jump risk.

We choose to hedge the jump risk by adding single option to the set of hedging instruments, i.e., we have $H_1(t) = S(t)$ and $H_2(t)$, which is a European option different from option $V_1(t)$ we aim to hedge. Option $H_2(t)$ is a risk-free option, such that no additional xVAs are introduced. To summarize, we have:

$$\Pi(t) = V_1(t) + \eta_1(t)S(t) + \eta_2(t)H_2(t).$$

We choose stock position $\eta_1(t)$ such that the portfolio is delta-neutral, i.e., such that $\frac{\partial \Pi(t)}{\partial S} = 0$:

$$\eta_1(t) = -\frac{\partial V_1(t)}{\partial S} - \eta_2(t)\frac{\partial H_2(t)}{\partial S}.$$

This leaves the question of how to choose $\eta_2(t)$. We use analytical jump parameter sensitivities to determine the remaining hedging position. As the strategy contains one hedging option, we must choose one of the jump parameters that we consider most important. All jump parameters have a level effect, μ_J also affects the skew, and σ_J also affects the curvature, see A.2. The level effect from ξ_J is more significant than that for μ_J and σ_J. Hence, we choose ξ_J to set up the hedge. So, for $\eta_2(t)$ we have:

$$\eta_2(t) = -\frac{\partial V_1(t)}{\partial \xi_J}\left[\frac{\partial H_2(t)}{\partial \xi_J}\right]^{-1}. \tag{4.9}$$

The partial derivatives w.r.t. ξ_J are computed analytically using the result in Eq. (A.2). The hedging strategy as presented here is equivalent to first taking a position in the stock $\eta_1(t)$ to hedge the trading instrument (so Eq. (4.6) but with the Merton delta), then taking position (4.9) to hedge the jump risk, and then updating $\eta_1(t)$ to account for the additional delta risk generated by this position in the hedging option.

5. Numerical results

We implement the market simulation, as introduced in Section 4, in a Monte Carlo setting. The algorithm used to obtain the numerical results is summarized below (Algorithm 1). All results are obtained with the following parameters: $t_0 = 0$,

Input: Trading strategies Π^{NoCCR} and Π^{CCR}, risk factors γ, number of simulation paths L and dates K
Output: Numerical results of the CVA hedging exercise

Initialize two portfolios Π^{NoCCR} and Π^{CCR}
Initialize simulation grid of risk factors γ
for $l \leftarrow 1$ **to** L **do**
  for $k \leftarrow 1$ **to** K **do**
    Simulate all risk factors $\gamma(t_k)$ for path l
    Re-value $\Pi^{\text{NoCCR}}(t_k)$ and $\Pi^{\text{CCR}}(t_k)$ for path l
    for $i \leftarrow 1$ **to** N **do**
      Re-value $V_i(t_{k-1}, \gamma(t_k))$ for path l to be used later in the $P\&L$ calculations
    end for
    for $j \leftarrow 1$ **to** M **do**
      Re-value $H_j(t_{k-1}, \gamma(t_k))$ for path l to be used later in the $P\&L$ calculations
    end for
  end for
  Simulate default time τ_l
  Perform closeout at default time τ_l for Π^{CCR}
  for $k \leftarrow 1$ **to** K **do**
    Compute the relevant $P\&L$ quantities at time t_k, prepare $P\&L_E$ for path l
    Compute wealth w^{NoCCR} and w^{CCR} for path l
  end for
end for
Compute required output metrics and visualize results

Algorithm 1: CVA hedging algorithm.

$T = 1$, $S(t_0) = 100$, $r = 0.1$, $\sigma = 0.2$, $K = 95$, $\xi_{\mathcal{P}} = 0.2$, and $R = 0.5$. For the Merton jump-diffusion parameters we choose $\sigma_J = 0.1$, $\mu_J = -0.125$, and $\xi_J = 0.1$, which can be interpreted as a jump of average size -11.3% that is expected every 10 years. We use $L = 10^5$ Monte Carlo paths and 200 time steps per year to create the set of monitoring dates. The results are

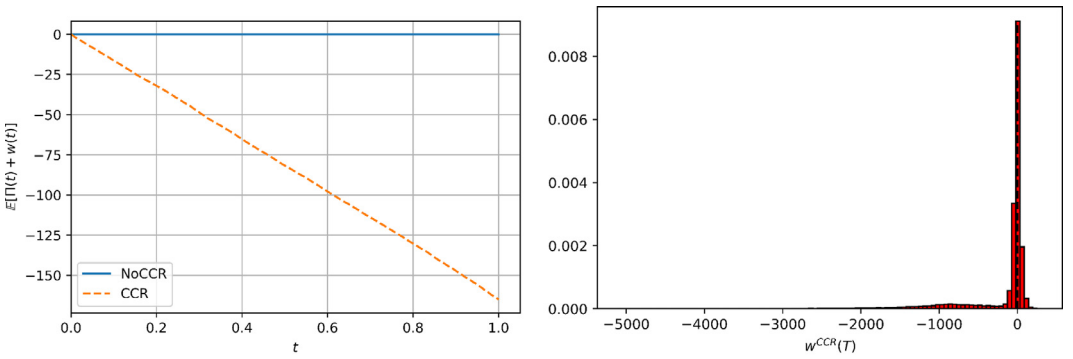

(a) Average $\Pi(t)$ and $w(t)$. (b) Distribution of w^{CCR} at maturity.

Fig. 1. CVA not included in the portfolio.

displayed using a number of 100 shares for the option, such that the controlled notional by the option is 10^4. As a result, the vertical axes of the plots can be interpreted as errors in bps. Furthermore, in the results the bank is represented as a single entity, meaning that the trading desk and xVA desk do not have separate trading strategies and wealth accounts. This split in the results can easily be made using the schematic drawings in Appendix C, but here we do not do this for sake of brevity.

5.1. Hedging CVA in a black-Scholes setting

The first numerical results correspond to the Black-Scholes hedging setting as discussed in Section 4.3. The Black-Scholes model is used for market simulation, computing hedging quantities, and *P*&*L* explain. First, we find that CVA must be charged to the client at trade inception to prevent an expected loss of the strategy. However, this CVA charge should not be treated as merely a cash amount, which ignores the impact of changes in the underlying market on the CVA through time. The $P\&L_P$ volatility resulting from the simulation seems to explode as the maturity date is approached. This behaviour can be understood through a set of analytical results that allow to interpret this phenomenon. We conclude that hedging the market risk of the CVA significantly reduces the $P\&L_P$ volatility, and that therefore CVA market risk must be hedged.

5.1.1. CVA As a cash amount

In Fig. 1a we confirm an expected loss at maturity if the counterparty could default, but no CVA is charged. This is done by examining the impact of simulated defaults on the portfolio, where an expected loss is represented by $\mathbb{E}_{t_0}[\Pi^{\mathrm{CCR}}(t_K) + w^{\mathrm{CCR}}(t_K)] < 0$. For Π^{NoCCR} we have the desired result, namely $\mathbb{E}_{t_0}[\Pi^{\mathrm{NoCCR}}(t_K) + w^{\mathrm{NoCCR}}(t_K)] \approx 0$, with some residual noise coming from the Monte Carlo simulation. The terminal wealth distribution in Fig. 1b can be interpreted as a bimodal distribution. The large peak corresponds to the paths without default, whereas the low and wide peak on the left corresponds to the losses encountered as a result of defaults.

Intuitively, $\mathbb{E}_{t_0}[\Pi^{\mathrm{CCR}}(t_K) + w^{\mathrm{CCR}}(t_K)] \approx \mathrm{CVA}(t_0)\dfrac{B(t_K)}{B(t_0)}$ should hold. Hence, we add the CVA charge at inception as a cash amount to the wealth account, meaning that we perform a linear shift in initial wealth. This should result in $\mathbb{E}_{t_0}[\Pi^{\mathrm{CCR}}(t_K) + w^{\mathrm{CCR}}(t_K)] \approx 0$, which is indeed the case, see Fig. 2a. So, the CVA charge proves to be a fair compensation of the credit riskiness of the counterparty. Furthermore, we see in Fig. 2b that the distribution of $w^{\mathrm{CCR}}(t_K)$ gets shifted to the right due to the CVA charge added at inception. The shift is precisely the required amount such that the mean of the distribution is around zero.

We see that charging the CVA at inception to the client and putting it on the wealth account overcomes the issue of an expected loss. However, treating the CVA charge as a cash number with no dependencies on underlying market variables is not useful in practice and naive. In practice, the CVA is charged to the client at trade inception. As time passes, changes in the market result in a change in CVA.

5.1.2. CVA Driven by market risk

Next, we consider the CVA to be driven by market risk, but we decide not to hedge this risk. This means we use the hedging quantity from Eq. (4.6) with the risk-free Black-Scholes delta, even though we have $V_1(t) = V(t) - \mathrm{CVA}(t)$.

Fig. 3 a represents the case in which CVA was added to the portfolio but not hedged. We see that the expected terminal wealth condition $\mathbb{E}_{t_0}[\Pi(t_K) + w(t_K)] = 0$ is satisfied. In Fig. 3b, we see that the variability of $\Pi(t) + w(t)$ for Π^{CCR} is much higher compared to that of Π^{NoCCR}. This is expected as a result of the additional source of randomness introduced by the simulated defaults in Π^{CCR}. $\Pi(t) + w(t)$ must always be examined first when assessing the performance of the portfolio, but it does not guarantee optimal performance.

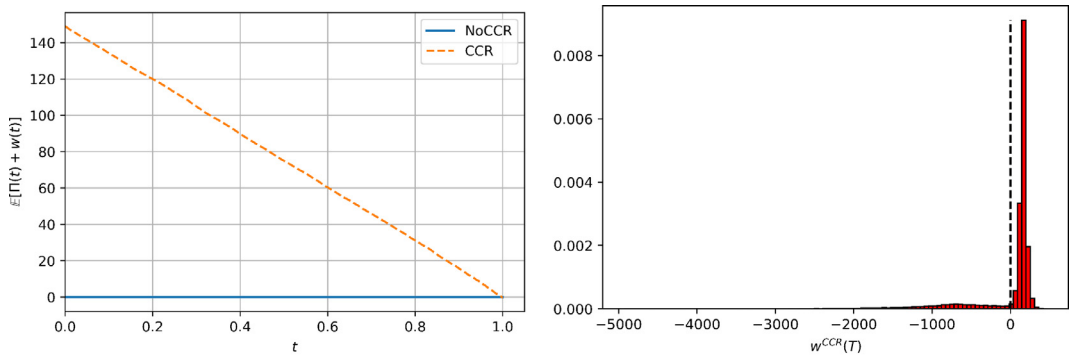

(a) Average $\Pi(t)$ and $w(t)$. (b) Distribution of w^{CCR} at maturity.

Fig. 2. CVA included in the portfolio as a cash amount.

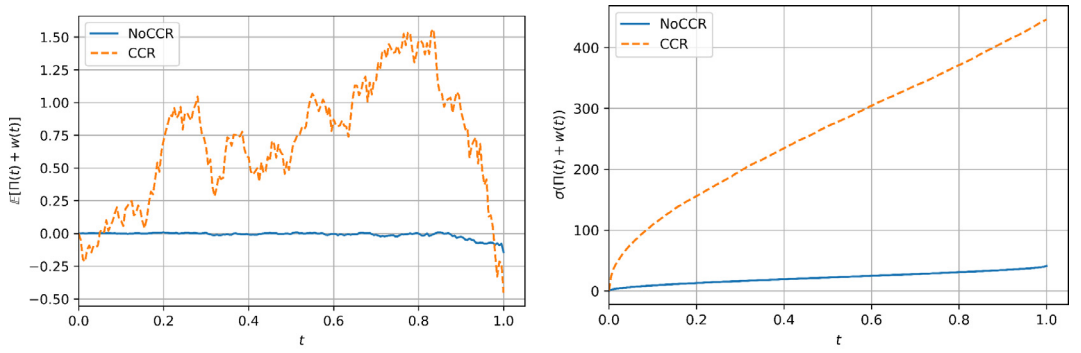

(a) Average $\Pi(t)$ and $w(t)$. (b) Volatility of $\Pi(t)$ and $w(t)$.

Fig. 3. Comparison of Π^{NoCCR} and Π^{CCR} using a Black-Scholes market and valuation model. CVA is not hedged.

Therefore, consider Figs. 4a and 4b, where we plot the mean and volatility of $P\&L_P(t)$. One can clearly see that even though the mean $P\&L_P$ for Π^{CCR} is slightly lower compared to Π^{NoCCR}, the volatility is significantly higher over the majority of the lifetime of the option. Thus, this hedging strategy is incomplete. The two lines in Fig. 4b overlap close to maturity, because the binarity of the payoff takes over. Furthermore, most of the simulated defaults have occurred by this time. Because after a default the same deal is entered with a credit risk free counterparty, the two portfolios eventually exhibit similar behaviour. From Figs. 4c and 4d we see that a significant portion of the $P\&L_P(t)$ can be explained using the underlying stock. [12] We see that the potential defaults through the lifetime of the option contribute to a significant initial difference in $P\&L_U$. This difference diminishes over time, as fewer defaults are expected to occur before the maturity of the option. As the strong increase in variance is not promising at a first glance, in Section 5.1.3 a thorough analysis of this behaviour can be found. All in all, the results indicate that CVA needs to be hedged to eliminate the majority of the underlying risk in the portfolio.

Looking at Fig. 4a, one might question why the average $P\&L_P(t_0)$ for Π^{NoCCR} is not equal to zero, as this would mean that a Black-Scholes delta hedge is unable to hedge all the risk of the option. Fig. 5a shows that this number converges to zero if $\mathrm{d}t \to 0$, so our observations are merely the result of the discretization. The volatility of $P\&L_P(t_0)$ for Π^{NoCCR} also converges to zero if the number of time-steps in the discretization is increased.

We also confirm that the CVA charged initially covers the otherwise experienced expected loss at default. We do this by showing that the following error measure is approximately zero:

$$\begin{aligned}\varepsilon(t_0) &= \mathbb{E}_{t_0}\left[1_{\{\tau \le t_K\}}\left[\frac{B(t_0)}{B(\tau)}(R \cdot V(\tau) - V(\tau)) + \text{CVA}(t_0)\right] + 1_{\{\tau > t_K\}}\text{CVA}(t_0)\right] \\ &\approx \frac{1}{L}\sum_{l=1}^{L} 1_{\{\tau_l \le t_K\}}\left[\frac{B(t_0)}{B(\tau_l)}(R \cdot V(\tau_l) - V(\tau_l)) + \text{CVA}(t_0)\right] + 1_{\{\tau_l > t_K\}}\text{CVA}(t_0), \end{aligned} \tag{5.1}$$

[12] In case a delta hedge was employed to hedge first order risks, this term was ignored in the $P\&L$ explain process to avoid taking the delta effect into account twice.

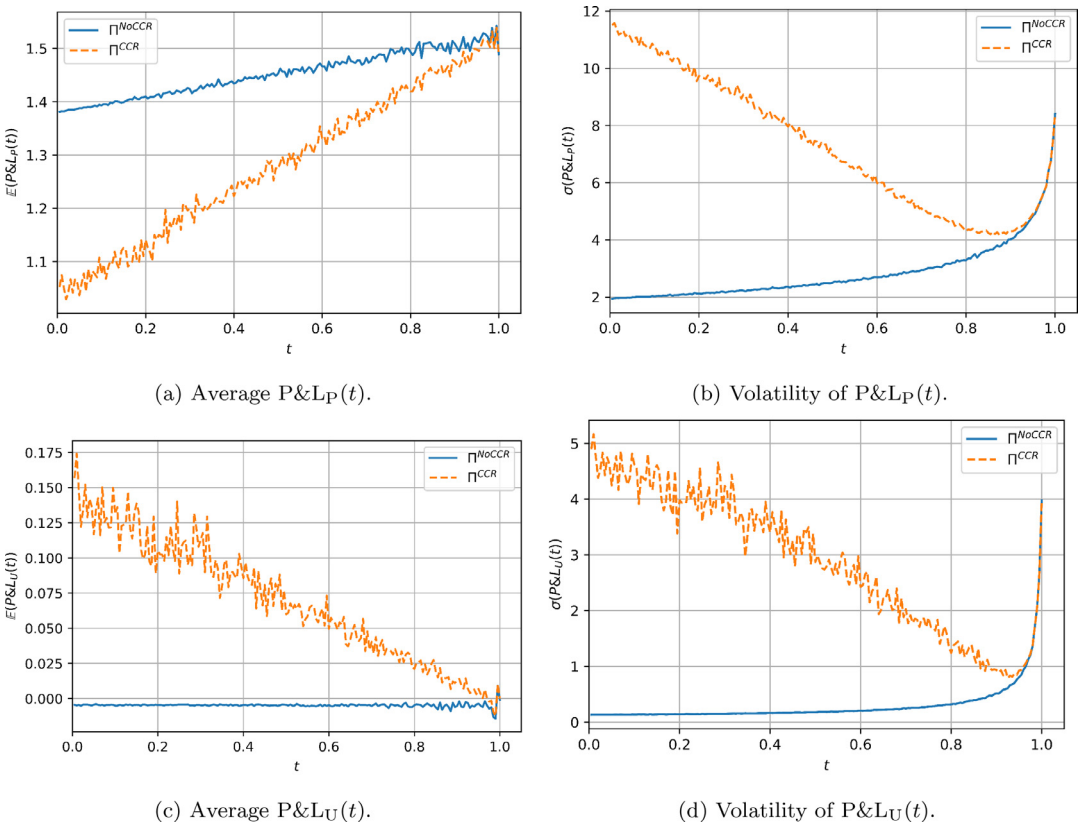

(a) Average $P\&L_P(t)$. (b) Volatility of $P\&L_P(t)$.

(c) Average $P\&L_U(t)$. (d) Volatility of $P\&L_U(t)$.

Fig. 4. Comparison of Π^{NoCCR} and Π^{CCR} using a Black-Scholes market and valuation model. CVA is not hedged.

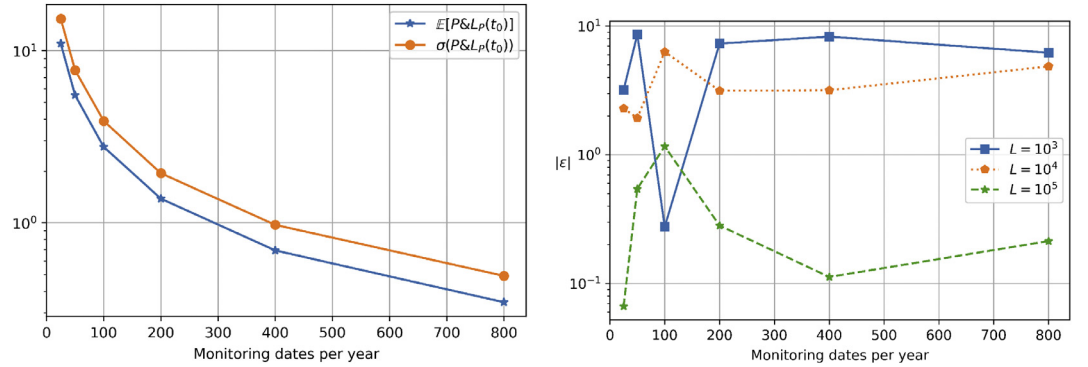

Fig. 5. (a) Π^{NoCCR} results of $P\&L_P(t_0)$ average and volatility for different number of monitoring dates, $L = 10^5$. (b) $|\varepsilon(t_0)|$ for different number of monitoring dates, per different number of Monte Carlo paths L.

where L denotes the number of Monte Carlo paths used in the simulation. We analyze the behaviour of this error measure by changing the number of Monte Carlo paths and number of time-steps used in the simulation. From Fig. 5b we see that for a given number of monitoring dates per year, increasing the number of paths results in $|\varepsilon(t_0)| \to 0$. Here we clearly see that using $L = 10^3$ provided unstable results, but we do observe converging behaviour when increasing L. As defaults occur infrequently, the number of paths must be large to properly approximate the numerical expectation from Eq. (5.1). Furthermore, the choice of 200 monitoring dates per year appears to be a very fine tradeoff between speed and accuracy.

5.1.3. Variance analysis

In Fig. 4b we see an exploding behaviour in the volatility of $P\&L_P$ as $t \to T$, for both Π^{NoCCR} and Π^{CCR}, which we want to understand. Therefore, we explain the distribution features we observe by looking at the $P\&L_P$ mean and variance for Π^{NoCCR}. Thus, we examine $P\&L_P$ for the portfolio in Eq. (4.3), with the Black-Scholes delta hedging quantity as in Eq. (4.6).

$P\&L_P$ from Eq. (3.10) with $\gamma(t) = S(t)$ can be rewritten as follows:

$$\begin{aligned} P\&L_P(t_k) &= \Pi(t_{k-1}, S(t_k)) - \Pi(t_{k-1}, S(t_{k-1})) \\ &= [V_1(t_{k-1}, S(t_k)) - V_1(t_{k-1}, S(t_{k-1}))] + \eta_1(t_{k-1})[S(t_k) - S(t_{k-1})]. \end{aligned} \tag{5.2}$$

Dividing both sides of Eq. (5.2) by $\mathrm{d}S = S(t_k) - S(t_{k-1})$, and using the definition of a forward finite difference approximation yields:

$$\begin{aligned} \frac{P\&L_P(t_k)}{S(t_k) - S(t_{k-1})} &= \frac{V_1(t_{k-1}, S(t_k)) - V_1(t_{k-1}, S(t_{k-1}))}{S(t_k) - S(t_{k-1})} - \frac{\partial V_1(t_{k-1})}{\partial S} \\ &= \frac{\mathrm{d}S}{2} \frac{\partial^2 V_1(t_{k-1}, S(t_{k-1}))}{\partial S^2} + \mathcal{O}\big((\mathrm{d}S)^2\big), \end{aligned} \tag{5.3}$$

(5.3)

$$\Rightarrow P\&L_P(t_k) = \frac{(\mathrm{d}S)^2}{2} \frac{\partial^2 V_1(t_{k-1}, S(t_{k-1}))}{\partial S^2} + \mathcal{O}\big((\mathrm{d}S)^3\big). \tag{5.4}$$

Eq. (5.4) shows that two types of errors drive $P\&L_P$. First, there is the truncation error of the forward finite differences which are used in Eq. (5.3). Furthermore, there is a discretization error that disappears if $\mathrm{d}S \to 0$, which will happen if $\mathrm{d}t = t_k - t_{k-1} \to 0$.

In Eq. (5.4), we recognize the second partial derivative as the option gamma, which under the Black-Scholes model is given by the following analytic expression:

$$\begin{aligned} \frac{\partial^2 V_1(t,S)}{\partial S^2} &= K\mathrm{e}^{-r(T-t)} \frac{\phi(d_2(t,S))}{S^2 \sigma \sqrt{T-t}}, \\ d_2(t,S) &= \frac{\ln \frac{S}{K} + \big(r - \frac{1}{2}\sigma^2\big)[T-t]}{\sigma\sqrt{T-t}}. \end{aligned} \tag{5.5}$$

Define $X \sim \mathcal{N}(\mu_X, \sigma_X^2)$ such that $S(t_k) \overset{\mathrm{d}}{=} S(t_{k-1})\mathrm{e}^X$, see Appendix B for further details. Using this and the Black-Scholes gamma (5.5), we rewrite Eq. (5.4) as follows:

$$\begin{aligned} P\&L_P(t_k) &= \frac{(\mathrm{d}S)^2}{2} K\mathrm{e}^{-r\tau} \frac{\phi(d_2(t_{k-1}, S(t_{k-1})))}{S^2(t_{k-1})\sigma\sqrt{\tau}} + \mathcal{O}\big((\mathrm{d}S)^3\big) \\ &= \frac{S^2(t_{k-1})\big[\mathrm{e}^X - 1\big]^2}{2} K\mathrm{e}^{-r\tau} \frac{\phi(d_2(t_{k-1}, S(t_{k-1})))}{S^2(t_{k-1})\sigma\sqrt{\tau}} + \mathcal{O}\big((\mathrm{d}S)^3\big) \\ &= \frac{K\mathrm{e}^{-r\tau}}{2\sigma\sqrt{\tau}}\big[\mathrm{e}^X - 1\big]^2 \phi(d_2) + \mathcal{O}\big((\mathrm{d}S)^3\big), \end{aligned} \tag{5.6}$$

where $\tau := T - t_{k-1}$ and for ease of notation we write $d_2 = d_2(t_{k-1}, S(t_{k-1}))$.

Define $d_2 \sim \mathcal{N}(\mu_{d_2}, \sigma_{d_2}^2)$, see Appendix B. Then, using definitions (B.13) and (B.14) for respectively $f(\mu_X, \sigma_X)$ and $g(\mu_X, \sigma_X)$, we obtain this expression of the variance of $P\&L_P$:

$$\mathbb{V}\mathrm{ar}_{t_0}(P\&L_P(t_k)) \approx \frac{K^2\mathrm{e}^{-2r\tau}}{8\pi\sigma^2\tau} \left[f(\mu_X, \sigma_X) \cdot \frac{\mathrm{e}^{-\frac{\mu_{d_2}^2}{1+2\sigma_{d_2}^2}}}{\sqrt{1+2\sigma_{d_2}^2}} - g(\mu_X, \sigma_X) \cdot \frac{\mathrm{e}^{-\frac{\mu_{d_2}^2}{1+\sigma_{d_2}^2}}}{1+\sigma_{d_2}^2} \right]. \tag{5.7}$$

See Appendix B for a full derivation of this result.

From Fig. 6 we see that the analytical result from Eq. (5.7) and volatility from the Monte Carlo simulation are in line. The strong increase of $P\&L_P$ volatility close to maturity can be understood from the perspective of $P\&L_P$ being driven by the option gamma, see Eq. (5.4). It is known for the option delta to be unstable near maturity, causing an increased gamma. This explains the increase in variance of $P\&L_P(t_k)$ as $t_k \to T$. Especially when the option is close to the ATM point, the gamma is large, causing a large gamma volatility.

Looking at Eq. (5.7), the strong increase in volatility towards maturity can be explained by looking at the variance as a scaled difference between the factors $\left(\sqrt{1+2\sigma_{d_2}^2}\right)^{-1}$ and $\left(1+\sigma_{d_2}^2\right)^{-1}$. The first term is non-linear, while the second is linear. Approaching maturity, the non-linearity of $\left(\sqrt{1+2\sigma_{d_2}^2}\right)^{-1}$ increases, causing the increased variance.

5.1.4. Hedging CVA

In Section 5.1.2 we concluded that CVA market risk needs to be hedged. Hence, we do so using the underlying stock, summarized by the hedging quantity Eq. (4.7).

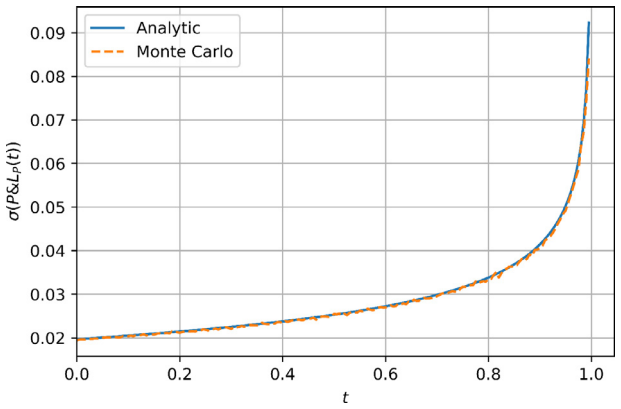

Fig. 6. Numerical confirmation that the analytical variance for Π^{NoCCR} from Eq. (5.7) is in line with the Monte Carlo simulation.

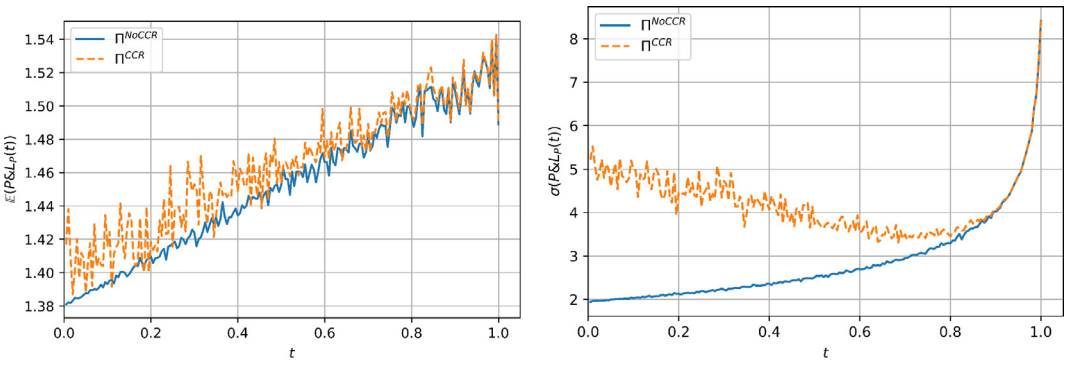

(a) Average $\text{P\&L}_\text{P}(t)$. (b) Volatility of $\text{P\&L}_\text{P}(t)$.

Fig. 7. Comparison of Π^{NoCCR} and Π^{CCR} using a Black-Scholes market and valuation model. CVA is hedged using the underlying stock.

In terms of the zero average return, hedging the CVA yields the same results as not hedging. Comparing Figs. 4a and 7a shows that the average $P\&L_P$ for Π^{CCR} is initially lower for the case where we do not hedge the CVA than when we do. However, this difference is not significant, especially not when taking the size of the volatility into consideration. In other words, the volatility appears to be a dominating factor in these results. Comparing Figs. 4b and 7b shows a benefit of hedging the CVA, as this yields a significantly lower volatility in $P\&L_P$. Hence, we confirm that CVA market risk must be hedged.

Regarding the $P\&L_U$, the results from Figs. 4c and 4d also hold for the situation with CVA market risk hedge. This makes sense, as the CVA market risk is either hedged and then does not need to be explained, or it is not hedged but then could be explained. So, hedging CVA market risk does not affect the result of how much $P\&L$ can be explained. The residual risk that remains after the $P\&L$ explain is illustrated by the differences between Π^{NoCCR} and Π^{CCR} in Figs. 4c and 4d. As suggested at the start of Section 4, CDSs can be added to the set of hedging instruments to hedge this jump risk at default, rather than only warehousing the credit risk.

5.2. Hedging CVA in a merton jump-diffusion setting

The numerical results in this section correspond to the Merton jump-diffusion hedging setting from Section 4.4. The Merton jump-diffusion model is used for market simulation, computing hedging quantities, and $P\&L$ explain. We show that when the stock is driven by a model that includes both jump and diffusion risk, the risk-free value of the trading instrument will be driven by these risks, but the same holds for the CVA component. Consequently these effects need to be taken into account when constructing the hedging positions.

Remark Instead of using the hedging strategy from Section 4.4, a delta hedge could be employed, for example like the Black-Scholes delta hedge as in Section 4.3, even though the market does not follow these dynamics. [13] We find that the Black-Scholes delta is unable to cope with jumps close to maturity, especially when an option is close to the ATM point and

[13] This is done by extracting the Black-Scholes implied volatility from the Merton option prices observed in the market, and setting up a Black-Scholes delta hedge using the underlying stock.

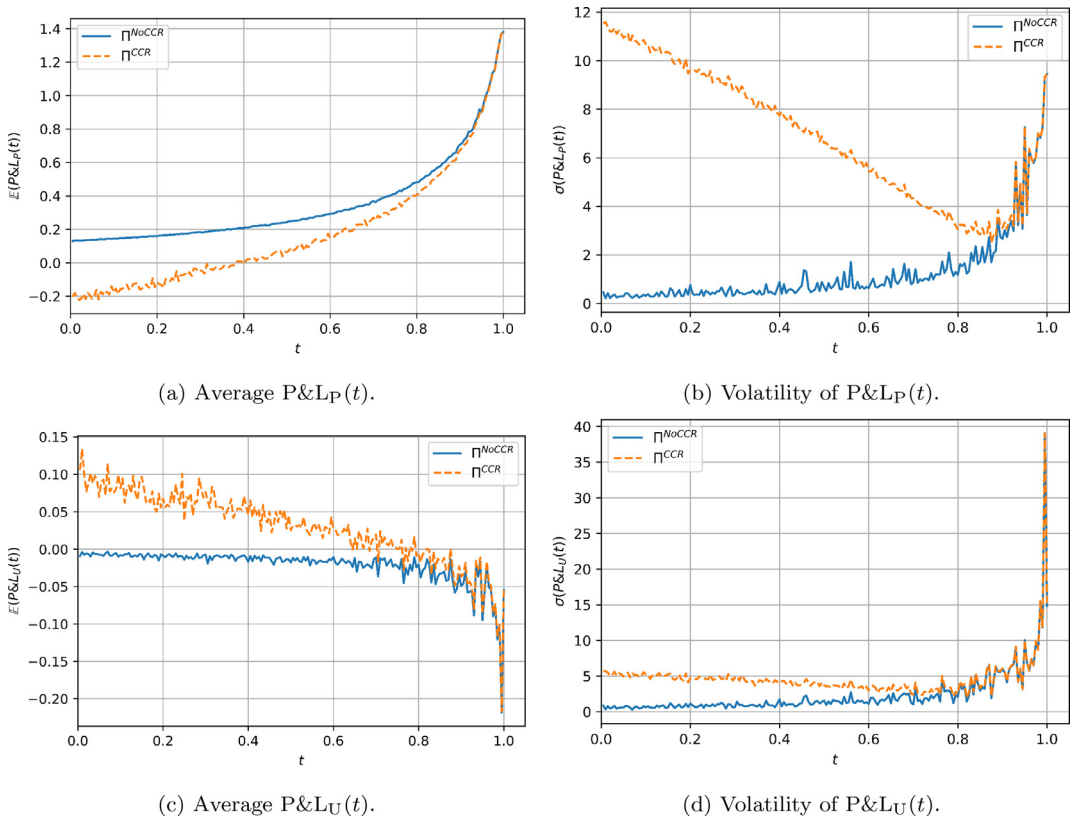

(a) Average $P\&L_P(t)$. (b) Volatility of $P\&L_P(t)$.

(c) Average $P\&L_U(t)$. (d) Volatility of $P\&L_U(t)$.

Fig. 8. Comparison of Π^{NoCCR} and Π^{CCR} using a Merton market and valuation model. An additional option is added to the hedging portfolio. CVA is not hedged.

a jump that triggers a change in moneyness. As a result, the gamma explain has an adverse effect, drastically increasing the $P\&L_U$ volatility. Clearly, the jump effects are missing in the explain process. The CVA hedge still has the same effect as before, putting aside the randomness from the stock jumps. We confirm the results by Naik and Lee [31] that this hedging strategy is not suitable for the case of an underlying asset driven by both diffusion and jump risk.

Alternatively, the Merton delta, as in Eq. (A.3), can be used to compute the hedging quantity. Eqs. (4.6) and (4.7) still hold in this case, given that the Black-Scholes deltas are replaced by Merton deltas. As a result, the instability close to maturity around the ATM point for the Black-Scholes delta hedge are no longer observed. Yet, the second order instability remains. Again, the CVA hedge has the same desired effect. As issues remain for the Merton delta hedge, additional hedging instruments need to be added to the strategy to cope with the additional randomness introduced by the stock jumps. This motivates the hedging strategy introduced in Section 4.4.

5.2.1. Hedging the jump risk using an option

We hedge the additional jump risk from the Merton model using an extra instrument in the hedging portfolio: one extra option. Typically, OTM options are chosen in the hedging portfolio as they are cheap. One of the difficulties resulting from Eq. (4.9) is that $\frac{\partial H_2(t)}{\partial \xi_j}$ tends to zero close to maturity, due to the option being OTM. $\frac{\partial V_1(t)}{\partial \xi_j}$ may behave the same, however, it is likely that $\frac{\partial H_2(t)}{\partial \xi_j}$ will decay faster due to the option being deeper OTM. As a result, $\eta_2(t)$ in Eq. (4.9) will increase drastically close to maturity of the option. For the hedging option we choose an OTM put with strike $K = 90$, maturity $T = 1$ and controlling the same number of shares as the original option we hedge. [14] In case we hedge the CVA, this is done using both the underlying stock and same option we use to hedge the product itself.

The desired effect of the single option hedge is clearly visible in the volatility of $\Pi(t) + w(t)$ for Π^{NoCCR}, which is similar to the Black-Scholes results from Fig. 3b. This means that a single option is already well equipped to mitigate a large portion of the jump risk in the stock. For Π^{CCR}, the CCR still dominates the jumps in the stock.

The mean $P\&L_P$ in Fig. 8a exhibits non-linear behaviour due to the additional optionally in the portfolio. The $P\&L_P$ volatility in Fig. 8b is comparable to the Black-Scholes case (see Fig. 4b), which again demonstrates the effectiveness of the single hedging option. Without this instrument significantly more volatility is observed.

[14] Alternatively, a hedging strategy that rolls over a short term option position to hedge a long term option can be used, see for example [28].

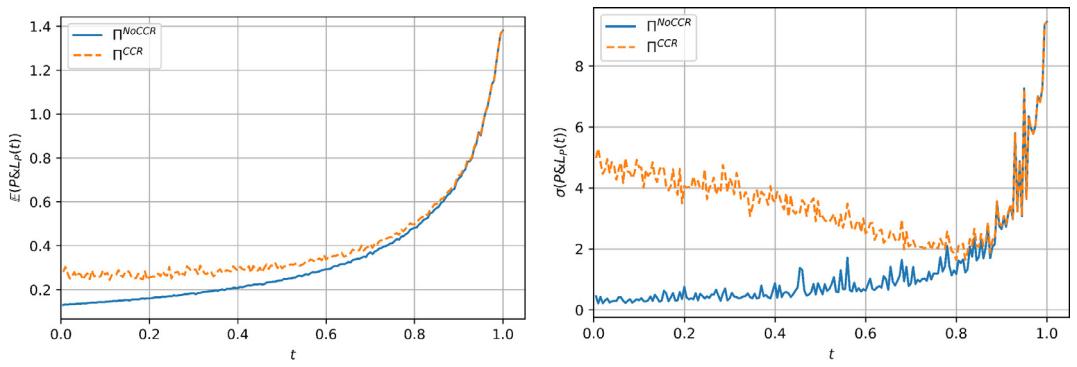

(a) Average $\mathrm{P\&L_P}(t)$. (b) Volatility of $\mathrm{P\&L_P}(t)$.

Fig. 9. Comparison of Π^{NoCCR} and Π^{CCR} using a Merton market and valuation model. An additional option is added to the hedging portfolio. CVA is hedged using both the underlying stock and the additional option.

The average $P\&L_U$ in Fig. 8c, is comparable to the Black-Scholes case up to the same non-linear effect we also observe for the $P\&L_P$. Overall, the volatility in Fig. 8d is comparable to the previous results for the Black-Scholes case (see Fig. 4d), except for a significantly higher peak just before maturity. This is the result of an exploding gamma explain volatility close to maturity.

The CVA hedge has no effect on $\Pi(t) + w(t)$ or $P\&L_U$, which is in line with our observations so far. The effect of the CVA hedge on $P\&L_P$, see Fig. 9, is similar to the effect in the Black-Scholes case (see Fig. 7). Especially the volatility, which is the dominating factor, is comparable to the Black-Scholes case (see Fig. 7b). For the average we observe in Fig. 9a that the Π^{CCR} is slightly above Π^{NoCCR}, which is also observed for the Black-Scholes case (see Fig. 7a).

Adding the option to the hedging strategy has the effect of smaller $P\&L_P$ volatility than when stock jump risk is present. Increasing the number of options in the hedging strategy will likely increase the hedging performance, however, the effect of the first option is already significant [28,29]. The increase in $P\&L_U$ volatility can be explained by the hedging option having a fixed strike. For some of the simulated paths, this hedge option may become significantly OTM, meaning the sensitivity to the jumps is close to zero. This results in a less effective hedge of the jump risk.

remark In addition to the experiments done so far, we perform the experiments under another set of parameters which represent a stressed market. For the Black-Scholes case we use an increased volatility of $\sigma = 0.35$. We observe the same patterns but with a different scaling of the results, all conclusions remain the same. For the Merton jump-diffusion case the stressed market is represented by the following choice of parameters: $\sigma_J = 0.2$, $\mu_J = -0.4$, and $\xi_J = 0.2$ This can be interpreted as a jump of average size -31.6% that is expected every 5 years, meaning we expect larger and more frequent jumps than before. When the stock jump risk is not hedged with an extra option, this risk dominates the CCR effect. This is no longer the case when adding an option to the set of hedging instruments. In general we observe comparable patterns, and an increase in level with more variability due to the increased randomness in the stock dynamics. On the other hand, the $P\&L_U$ volatility is shifted upwards and the peak close to maturity increases significantly. So for this setting with larger and more frequent jumps, a single hedging option seems to be less sufficient to hedge the randomness in the stock. However, the effect of the CVA hedge remains unchanged.

6. Conclusion

In conclusion, dynamic hedging of CVA market risk is now better understood, both in a Black-Scholes and a Merton jump-diffusion setting. Starting from a theoretical hedging framework, we have examined the mechanics of a trading strategy which included CVA pricing and hedging. We visualized cash-flows and exchanges of traded instruments of the portfolio. For a case study of a portfolio containing European options and the underlying stock, we used a Monte Carlo simulation to study hedging. Hedging performance was assessed by analyzing the trading strategy balance, including the corresponding wealth account. Furthermore, we studied the $P\&L$ behaviour of the strategy, as well as the performance of the $P\&L$ explain. In particular, analytic results helped us to explain and analyze $P\&L$ behaviour that was observed from the simulation.

First, in a Black-Scholes setting we showed that failing to charge CVA to a credit risky counterparty will result in an expected loss, motivating the vision of CVA as fair compensation for this credit risk. We have shown that CVA market risk in a Black-Scholes context can satisfactorily be hedged using the underlying stock, resulting in an improved stability of the trading strategy in the form of a lower $P\&L_P$ volatility. For the $P\&L_P$, we saw a significant increase in volatility as the option maturity approached, which we understood as the result of gamma instability close to maturity. We conclude that CVA market risk hedging is necessary for a more stable trading strategy.

The residual risk after the CVA market risk hedge and *P&L* explain can be hedged using CDSs as opposed to the current credit risk warehousing. This will be interesting to study when taking into account Wrong Way Risk effects, for example by choosing a credit process dynamics which is correlated to the market risks. We leave this for future research.

Next, we examined our case study portfolio when the underlying stock is driven by a Merton jump-diffusion process. Adding an option as a hedging instrument mitigates a significant part of the jump risk. Hedging the CVA market risk in this situation is still a must. Extending the hedging instruments with more options may result in an even more stable strategy.

The framework can easily be extended for more advanced models for the stock dynamics like a stochastic (local) volatility model. This is relevant for exotic trading instruments, e.g., a path-dependent option. In this case, increase the number of hedging instruments, as now the model is calibrated to a full range of option strikes and maturities. Computing future exposures will require extra effort, but can be done working in a Least-Squares Monte-Carlo setting for example.

All in all, the theoretical hedging framework in which dynamic CVA hedging has been studied allows one to consider a broad selection of trading strategies, but above all different and more xVAs. Understanding the mechanics of CVA hedging is a crucial first step for future research on xVA hedging.

Acknowledgements

This work has been financially supported by Rabobank. The authors would like to thank the two anonymous referees for their helpful comments and feedback, which contributed to an improvement of the manuscript.

Appendix A. The Merton jump-diffusion model

A1. Analytical european option prices and sensitivities

Here we re-iterate a result from [7,27], namely the analytical expression for a European call option price on stock S, maturity T, and strike K, under the Merton jump-diffusion model:

$$\begin{aligned}
V(t) &= \mathrm{e}^{-r(T-t)} \sum_{n\geq 0} \frac{\left[\xi_J(T-t)\right]^n \mathrm{e}^{-\xi_J(T-t)}}{n!} \overline{V}(n), \qquad \text{(A.1)}\\
\overline{V}(n) &= \mathrm{e}^{\hat{\mu}_X(n)+\frac{1}{2}\hat{\sigma}_X^2(n)(T-t)}\Phi(d_1) - K\Phi(d_2),\\
\hat{\mu}_X(n) &= \log(S(t)) + \left[r - \xi_J\left(\mathrm{e}^{\mu_J+\frac{1}{2}\sigma_J^2}-1\right) - \frac{1}{2}\sigma^2\right](T-t) + n\mu_J,\\
\hat{\sigma}_X(n) &= \sqrt{\sigma^2 + \frac{n\sigma_J^2}{T-t}}, \quad d_2 = d_1 - \hat{\sigma}_X(n)\sqrt{T-t},\\
d_1 &= \frac{\log\left(\frac{S(t)}{K}\right) + \left[r - \xi_J\left(\mathrm{e}^{\mu_J+\frac{1}{2}\sigma_J^2}-1\right) - \frac{1}{2}\sigma^2 + \hat{\sigma}_X^2(n)\right](T-t) + n\mu_J}{\hat{\sigma}_X(n)\sqrt{T-t}},
\end{aligned}$$

where r is the risk-free interest rate, σ is the stock volatility. Furthermore, μ_J, σ_J, and ξ_J are respectively the jump mean, volatility and intensity. In the case of a put option, one can simply apply the *put-call parity* to the call option price from Eq. (A.1).

It can be shown that call price $V(t)$ from Eq. (A.1) has the following analytical expressions of derivatives w.r.t. jump intensity ξ_J:

$$\begin{aligned}
\frac{\partial V(t)}{\partial \xi_J} &= \mathrm{e}^{-r(T-t)} \sum_{n\geq 0} \frac{\left[\xi_J(T-t)\right]^n \mathrm{e}^{-\xi_J(T-t)}}{n!}\\
&\quad \left(\overline{V}(n)\left[\frac{n}{\xi_J} - (T-t)\right] - \left(\mathrm{e}^{\mu_J+\frac{1}{2}\sigma_J^2}-1\right)(T-t)\mathrm{e}^{\hat{\mu}_X(n)+\frac{1}{2}\hat{\sigma}_X^2(n)(T-t)}\Phi(d_1)\right). \qquad \text{(A.2)}
\end{aligned}$$

This result is valid for both call and put options, which can be seen from the put-call parity.

In a similar fashion we can derive the following expression for the call option *delta* and *gamma* under the Merton jump-diffusion model:

$$\frac{\partial V(t)}{\partial S} = \mathrm{e}^{-r(T-t)} \sum_{n\geq 0} \frac{\left[\xi_J(T-t)\right]^n \mathrm{e}^{-\xi_J(T-t)}}{n!} \cdot \mathrm{e}^{\hat{\mu}_X(n)-\log(S(t))+\frac{1}{2}\hat{\sigma}_X^2(n)(T-t)}\Phi(d_1), \qquad \text{(A.3)}$$

$$\frac{\partial^2 V(t)}{\partial S^2} = \mathrm{e}^{-r(T-t)} \sum_{n\geq 0} \frac{\left[\xi_J(T-t)\right]^n \mathrm{e}^{-\xi_J(T-t)}}{n!} \cdot \mathrm{e}^{\hat{\mu}_X(n)-\log(S(t))+\frac{1}{2}\hat{\sigma}_X^2(n)(T-t)} \frac{\phi(d_1)}{S(t)\hat{\sigma}_X(n)\sqrt{T-t}}, \qquad \text{(A.4)}$$

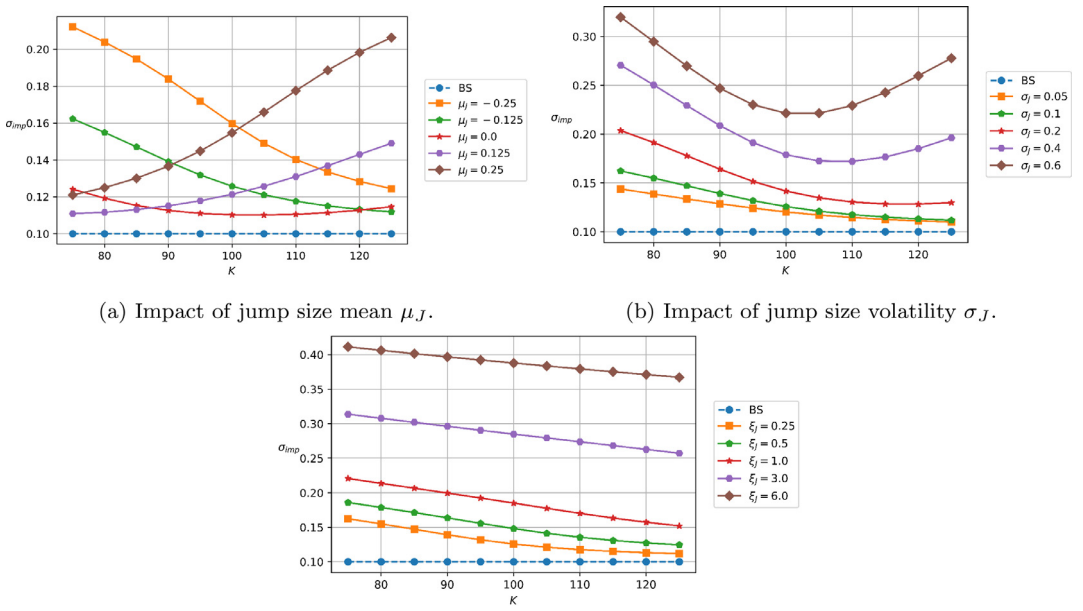

(a) Impact of jump size mean μ_J.

(b) Impact of jump size volatility σ_J.

(c) Impact of jump intensity ξ_J.

Fig. A1. Merton jump parameter impact on σ_{imp}. Parameters: $S(t_0) = 100$, $r = 0.05$, $\sigma = 0.1$, $t_0 = 0$, $T = 1$. Jump parameters base values: $\mu_J = -0.125$, $\sigma_J = 0.1$, $\xi_J = 0.25$. $\mu_J \in \{-0.25, -0.125, 0.0, 0.125, 0.25\}$, $\sigma_J \in \{0.05, 0.1, 0.2, 0.4, 0.6\}$, $\xi_J \in \{0.25, 0.5, 1.0, 3.0, 6.0\}$.

The option pricing formula (A.1) contains an infinite sum of scaled Black-Scholes option prices, being a direct result of the jump size following a continuous distribution. This clearly shows that if one attempts to hedge the jump risk introduced by the model, one would theoretically need infinitely many options to do so, which is infeasible from a practical perspective.

A2. Jump parameter impact on implied volatilities

We assess the impact of the jump parameters on the *Black-Scholes implied volatilities* σ_{imp}. We do so by varying parameters μ_J, σ_J, and ξ_J one by one while keeping all the others constant.

In Fig. A.10a we observe that μ_J has a *level effect*. In addition the *slope*, i.e., *skew*, and direction of the slope are affected. For the simulations we choose a negative value of μ_J, which implies that the stock will likely go down. The reason of this choice is that typically in the market we see that OTM options are cheaper, which matches the higher likelihood of a downward jump in stock. From Fig. A.10b we conclude that σ_J has an impact on both the level and the *curvature* of the implied volatility. A higher σ_J means more uncertainty, hence higher option prices, so also a higher σ_{imp}. The curvature effect can be observed by the OTM strike region exhibiting a more pronounced *hockey-stick* effect which becomes larger as σ_J increases. Finally, Fig. A.10c tells us that ξ_J impacts the level only. For higher ξ_J, jumps will occur more frequently, introducing more uncertainty, resulting in higher σ_{imp}.

Appendix B. Variance analysis derivations

As is stated in Section 5.1.3, we derive an analytic expression for the mean and variance of $P\&L_P$ from Eq. (5.6). But before that, we need the following two results. First,

$$\begin{aligned} S(t_k) \quad &\overset{\text{d}}{=} S(t_{k-1})\mathrm{e}^{X}, \\ X &= \left(r - \frac{1}{2}\sigma^2\right)[t_k - t_{k-1}] + \sigma\sqrt{t_k - t_{k-1}}Z \\ &\sim \mathcal{N}\left(\left(r - \frac{1}{2}\sigma^2\right)[t_k - t_{k-1}], \sigma^2[t_k - t_{k-1}]\right) =: \mathcal{N}(\mu_X, \sigma_X^2), \end{aligned} \tag{B.1}$$

where $Z \sim \mathcal{N}(0, 1)$. Second, in a similar fashion as Eq. (B.1) we write:

$$S(t_{k-1}) \overset{\text{d}}{=} S(t_0)\exp\left\{\left(r - \frac{1}{2}\sigma^2\right)[t_{k-1} - t_0] + \sigma\sqrt{t_{k-1} - t_0}\tilde{Z}\right\}, \tag{B.2}$$

where $\tilde{Z} \sim \mathcal{N}(0,1)$, independent of Z. Using Eq. (B.2) and $\tau := T - t_{k-1}$ we write d_2 as:

$$\begin{aligned} d_2 &= \frac{\ln \frac{S(t_0)}{K} + \left(r - \frac{1}{2}\sigma^2\right)[T-t_0]}{\sigma\sqrt{\tau}} + \sqrt{\frac{t_{k-1}-t_0}{\tau}}\tilde{Z} \\ &\sim \mathcal{N}\left(\frac{\ln \frac{S(t_0)}{K} + \left(r - \frac{1}{2}\sigma^2\right)[T-t_0]}{\sigma\sqrt{\tau}}, \frac{t_{k-1}-t_0}{\tau}\right) =: \mathcal{N}(\mu_{d_2}, \sigma_{d_2}^2). \end{aligned}$$

B1. Mean

We are interested in how $P\&L_P$ from Eq. (5.6) is distributed conditional on the information known at today (t_0). First, look at the mean:

$$\mathbb{E}_{t_0}[P\&L_P(t_k)] \approx \mathbb{E}_{t_0}\left[\frac{K\mathrm{e}^{-r\tau}}{2\sigma\sqrt{\tau}}\left[\mathrm{e}^X - 1\right]^2\phi(d_2)\right] = \frac{K\mathrm{e}^{-r\tau}}{2\sigma\sqrt{\tau}}\mathbb{E}_{t_0}\left[\left[\mathrm{e}^X - 1\right]^2\right]\mathbb{E}_{t_0}[\phi(d_2)], \tag{B.3}$$

where we use the independency of $\left[\mathrm{e}^X - 1\right]^2$ and $\phi(d_2)$ due to the independent increments. The first expectation from Eq. (B.3) can be written as:

$$\begin{aligned} \mathbb{E}_{t_0}\left[\left[\mathrm{e}^X - 1\right]^2\right] &= \mathbb{V}\mathrm{ar}_{t_0}\left(\mathrm{e}^X - 1\right) + \left(\mathbb{E}_{t_0}\left[\mathrm{e}^X - 1\right]\right)^2 \\ &= \left(\mathrm{e}^{\sigma_X^2} - 1\right)\mathrm{e}^{2\mu_X + \sigma_X^2} + \left(\mathrm{e}^{\mu_X + \frac{1}{2}\sigma_X^2} - 1\right)^2, \end{aligned} \tag{B.4}$$

where we use the lognormality of e^X. The second expectation can be written as:

$$\mathbb{E}_{t_0}[\phi(d_2)] = \frac{\mathbb{E}_{t_0}\left[\mathrm{e}^{-\frac{1}{2}d_2^2}\right]}{\sqrt{2\pi}} = \frac{\mathrm{e}^{-\frac{\mu_{d_2}^2}{2\left(1+\sigma_{d_2}^2\right)}}}{\sqrt{2\pi}\sqrt{1+\sigma_{d_2}^2}}, \tag{B.5}$$

where we use the fact that d_2^2 follows $\sigma_{d_2}^2$ times a non-central chi-squared distribution with one degree of freedom ($k = 1$), and with non-centrality parameter $\lambda = \frac{\mu_{d_2}^2}{\sigma_{d_2}^2}$, i.e., $d_2^2 \sim \sigma_{d_2}^2\chi^2\left(1, \frac{\mu_{d_2}^2}{\sigma_{d_2}^2}\right)$. Using results (B.4) and (B.5) allows us to rewrite Eq. (B.3) as:

$$\mathbb{E}_{t_0}[P\&L_P(t_k)] \approx \frac{K\mathrm{e}^{-r\tau}}{2\sigma\sqrt{\tau}}\frac{\mathrm{e}^{-\frac{\mu_{d_2}^2}{2\left(1+\sigma_{d_2}^2\right)}}}{\sqrt{2\pi}\sqrt{1+\sigma_{d_2}^2}}\left(\left(\mathrm{e}^{\sigma_X^2} - 1\right)\mathrm{e}^{2\mu_X + \sigma_X^2} + \left(\mathrm{e}^{\mu_X + \frac{1}{2}\sigma_X^2} - 1\right)^2\right). \tag{B.6}$$

B2. Variance

For the variance of $P\&L_P$ from Eq. (5.6) we have:

$$\mathbb{V}\mathrm{ar}_{t_0}(P\&L_P(t_k)) = \mathbb{E}_{t_0}\left[(P\&L_P(t_k))^2\right] - \left(\mathbb{E}_{t_0}[P\&L_P(t_k)]\right)^2, \tag{B.7}$$

where the second term can be computed using Eq. (B.6). By the independent increment argument, the first term in Eq. (B.7) can be written as:

$$\begin{aligned} \mathbb{E}_{t_0}\left[(P\&L_P(t_k))^2\right] &\approx \mathbb{E}_{t_0}\left[\left(\frac{K\mathrm{e}^{-r\tau}}{2\sigma\sqrt{\tau}}\left[\mathrm{e}^X - 1\right]^2\phi(d_2)\right)^2\right] \\ &= \frac{K^2\mathrm{e}^{-2r\tau}}{4\sigma^2\tau}\mathbb{E}_{t_0}\left[\left[\mathrm{e}^X - 1\right]^4\right]\mathbb{E}_{t_0}\left[(\phi(d_2))^2\right]. \end{aligned} \tag{B.8}$$

For the first expectation in Eq. (B.8) we write:

$$\begin{aligned} \mathbb{E}_{t_0}\left[\left[\mathrm{e}^X - 1\right]^4\right] &= \mathbb{E}_{t_0}\left[\mathrm{e}^{4X} - 4\mathrm{e}^{3X} + 6\mathrm{e}^{2X} - 4\mathrm{e}^X + 1\right] \\ &= \mathrm{e}^{4\mu_X + \frac{16}{2}\sigma_X^2} - 4\mathrm{e}^{3\mu_X + \frac{9}{2}\sigma_X^2} + 6\mathrm{e}^{2\mu_X + \frac{4}{2}\sigma_X^2} - 4\mathrm{e}^{\mu_X + \frac{1}{2}\sigma_X^2} + 1, \end{aligned} \tag{B.9}$$

using the properties of the moment generating function of X. The second expectation in Eq. (B.8) can be written as:

$$\mathbb{E}_{t_0}\left[(\phi(d_2))^2\right] = \frac{\mathbb{E}_{t_0}\left[\mathrm{e}^{-d_2^2}\right]}{2\pi} = \frac{\mathrm{e}^{-\frac{\mu_{d_2}^2}{1+2\sigma_{d_2}^2}}}{2\pi\sqrt{1+2\sigma_{d_2}^2}}, \tag{B.10}$$

where we once more use that d_2^2 follows $\sigma_{d_2}^2$ times a non-central chi-squared distribution with parameters as stated before. Results (B.9) and (B.10) allow us to rewrite Eq. (B.8) as:

$$\mathbb{E}_{t_0}\left[(P\&L_P(t_k))^2\right] \approx \frac{K^2 e^{-2r\tau}}{4\sigma^2\tau} \frac{e^{-\frac{\mu_{d_2}^2}{1+2\sigma_{d_2}^2}}}{2\pi\sqrt{1+2\sigma_{d_2}^2}} \left(e^{4\mu_X+\frac{16}{2}\sigma_X^2} - 4e^{3\mu_X+\frac{9}{2}\sigma_X^2} + 6e^{2\mu_X+\frac{4}{2}\sigma_X^2} - 4e^{\mu_X+\frac{1}{2}\sigma_X^2} + 1\right). \tag{B.11}$$

Using the results from Eqs. (B.6) and (B.11) in Eq. (B.7) yields:

$$\mathbb{V}\mathrm{ar}_{t_0}(P\&L_P(t_k)) \approx \frac{K^2 e^{-2r\tau}}{8\pi\sigma^2\tau} \left[f(\mu_X,\sigma_X)\cdot \frac{e^{-\frac{\mu_{d_2}^2}{1+2\sigma_{d_2}^2}}}{\sqrt{1+2\sigma_{d_2}^2}} - g(\mu_X,\sigma_X)\cdot \frac{e^{-\frac{\mu_{d_2}^2}{1+\sigma_{d_2}^2}}}{1+\sigma_{d_2}^2} \right], \tag{B.12}$$

where

$$f(\mu_X,\sigma_X) := e^{4\mu_X+\frac{16}{2}\sigma_X^2} - 4e^{3\mu_X+\frac{9}{2}\sigma_X^2} + 6e^{2\mu_X+\frac{4}{2}\sigma_X^2} - 4e^{\mu_X+\frac{1}{2}\sigma_X^2} + 1, \tag{B.13}$$

$$g(\mu_X,\sigma_X) := \left(\left(e^{\sigma_X^2}-1\right)e^{2\mu_X+\sigma_X^2} + \left(e^{\mu_X+\frac{1}{2}\sigma_X^2}-1\right)^2 \right)^2. \tag{B.14}$$

Appendix C. Desk structure and flow of cash

The simulation is illustrated by a series of schematic drawings that indicate the flow of cash and instruments. In all figures to follow, dotted lines indicate flows of cash, hence this relates to wealth accounts w, w^{trading}, and w^{xVA}. Furthermore, solid lines indicate the exchange of a product/asset, hence this relates to portfolios Π, Π^{trading}, and Π^{xVA}. Values are seen from the perspective of the desks, i.e., an arrow away from (towards) a desk indicates the desk needs to pay (receives). We assume that the wealth account at time t_{k-1} is positive, in the sense that this can be seen as a deposit with the Treasury department for which interest is received. [15]

We examine both the internal exchange of cash-flows and products between the trading desk and xVA desk, as well as the external exchange with the counterparty and other market entities. For the option and CVA market risk hedging quantity we write

$$\eta_1(t) = \underbrace{-\frac{\partial V(t)}{\partial S}}_{-\Delta(t)} + \underbrace{\frac{\partial V(t)}{\partial S}(1-R)\mathrm{PD}(t,t_K)}_{-\overline{\Delta}(t)}.$$

The situation at t_0 is displayed in Fig. C.11, where the positions in trading and hedging instruments are assumed. That is, the risky option V_1 is bought from the counterparty (blue lines) and both desks construct their market risk hedges (red and cyan lines). The transfer of the CVA between the trading and xVA desk, indicating that the trading desk manages the risk-free component of the transaction, whereas the xVA desk manages the CVA. In this example the xVA desk decides to actively manage the CVA market risk and warehouse the residual credit risk that can manifest itself upon the jump to default of the counterparty. When a default occurs this will result in a loss for the xVA desk, leaving the trading desk unaffected.

At $t_0 < t_k < t_K$, if there is no default, both desks rebalance their hedging positions (red and cyan lines) and receive interest from the Treasury department on their wealth account (teal lines). In case of a default at $t_0 < \tau = t_d < t_K$, see Fig. C.12, a risk-free closeout takes place between the bank and the counterparty (brown lines). [16] Again, we receive interest (teal lines), and the trading desk rebalances its hedging position on the option (red lines). Furthermore, the xVA desk enters the same risk-free contract V with a clearing house (violet lines) and closes its CVA hedging position (cyan lines). The xVA desk then gives the new contract V to the trading desk (violet lines), so that this desk is immune to the default. The 'damage' of the default is thus visible at the xVA desk level, which is precisely the place handling this risk.

Finally, Fig. C.13 represents the situation at t_K, at which interest is received (teal lines), the option payoff is settled in cash (violet lines), and the trading desk closes its hedging positions (red lines). The output metrics as introduced in Section 3.1 can be carefully analyzed to draw conclusions about the hedging strategy used.

[15] In the case that $w(t_{k-1})$ is negative we have to pay interest to the Treasury desk on the borrowed amount and the flows between the Treasury department and wealth account would be in the opposite direction.

[16] Here we assume the default takes place before maturity. The case of default at maturity is not discussed for sake of brevity. The remaining case naturally extends from the demonstrated material.

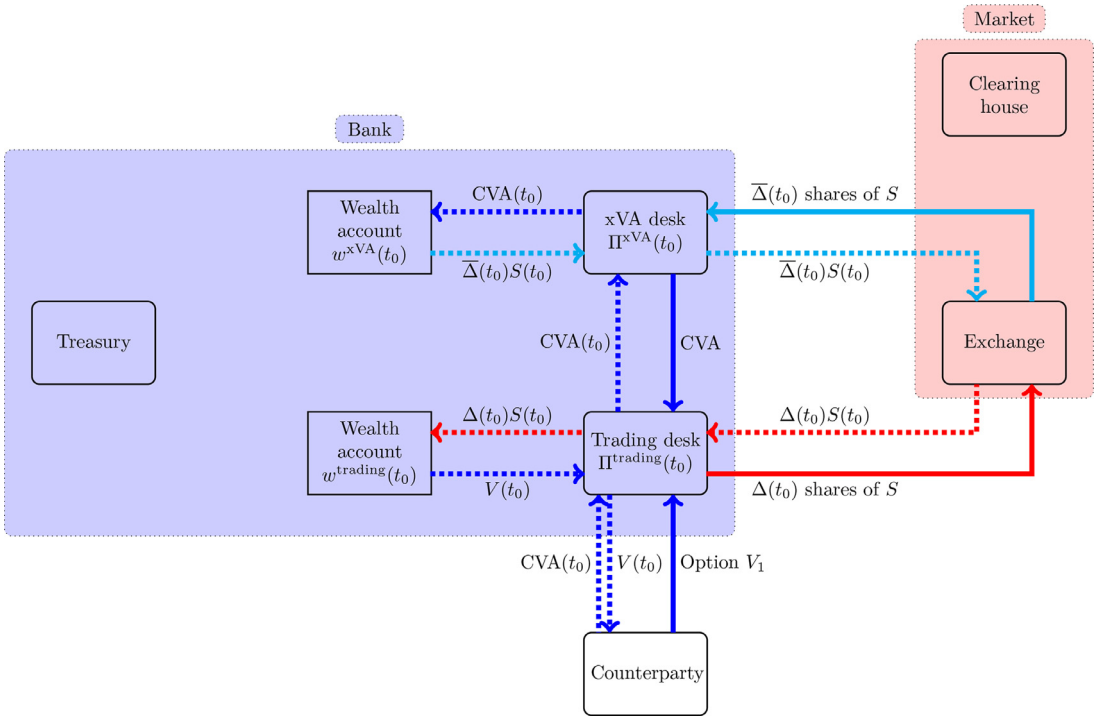

Fig. C1. Case with CCR, separate trading desk and xVA desk within the bank, situation at t_0. The blue lines correspond to the trade; the red lines correspond to the market risk hedge; the cyan lines correspond to the CVA market risk hedge. (For interpretation of the references to colour in this figure legend, the reader is referred to the web version of this article.)

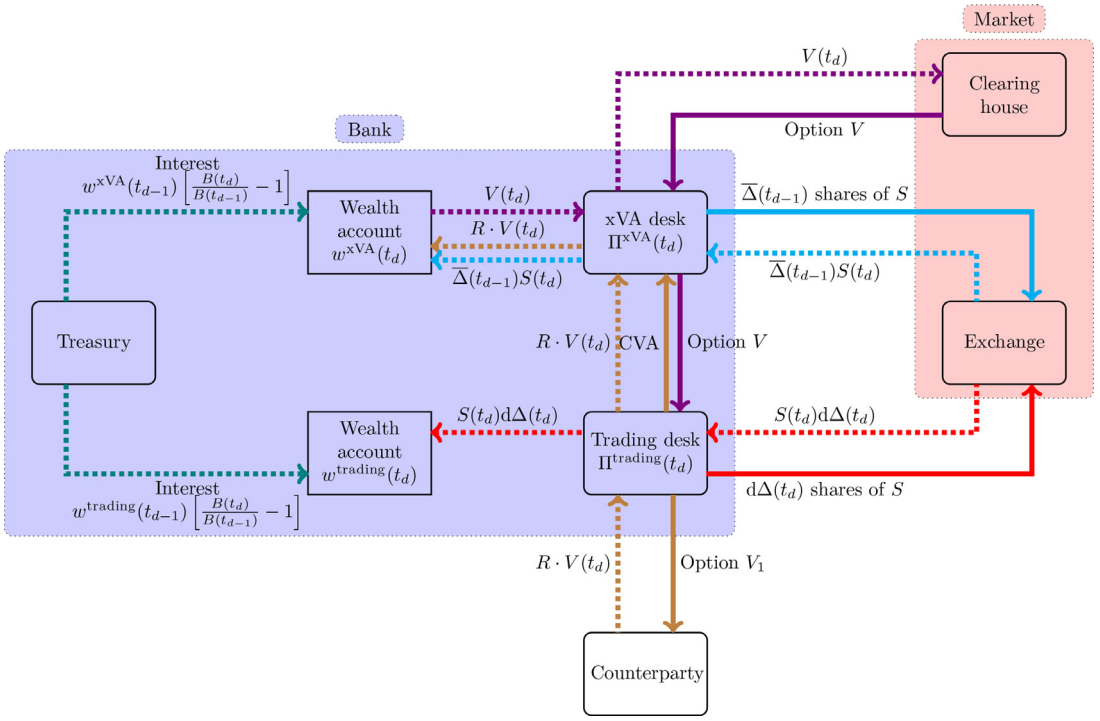

Fig. C2. Case with CCR, separate trading desk and xVA desk within the bank, situation at $t_0 < \tau = t_d < t_K$. The red lines correspond to the market risk hedge; the cyan lines correspond to the CVA market risk hedge; the teal lines correspond to the interest; the brown lines correspond to the default; the violet lines correspond to the new trade entered upon default. (For interpretation of the references to colour in this figure legend, the reader is referred to the web version of this article.)

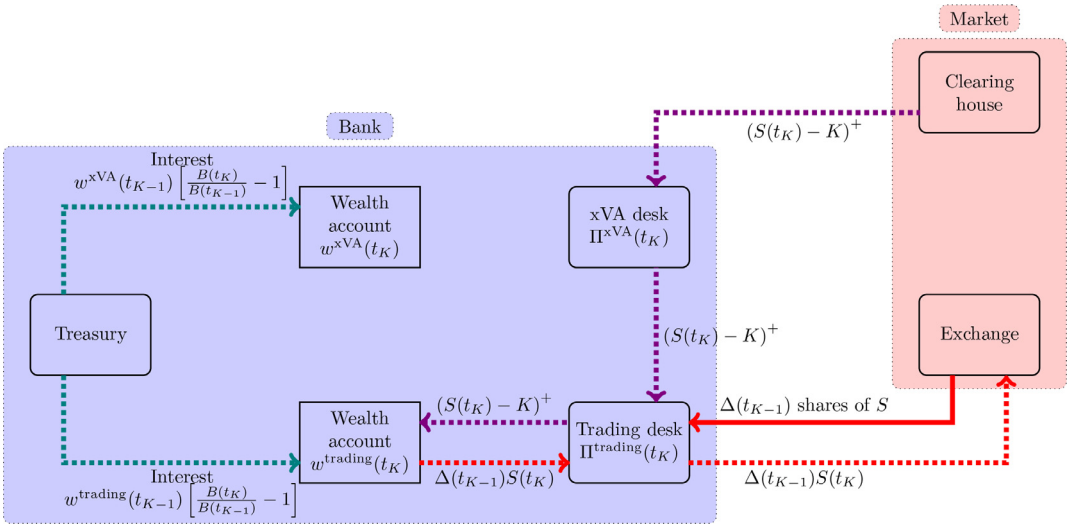

Fig. C3. Case with CCR, separate trading desk and xVA desk within the bank, situation at t_K. The red lines correspond to the market risk hedge; the teal lines correspond to the interest; the violet lines correspond to the cash settlement of the new trade entered upon default. (For interpretation of the references to colour in this figure legend, the reader is referred to the web version of this article.)

References

[1] A. Green, XVA: Credit, Funding and Capital Valuation Adjustments, first, Wiley Finance, 2015. ISBN 978-1-118-55678-8
[2] J. Gregory, The xVA Challenge - Counterparty Credit Risk, Funding, Collateral and Capital, third, Wiley Finance, 2015. ISBN 978-1-119-10941-9
[3] Basel committee on banking supervision, BIS, Capital treatment for bilateral counterparty credit risk finalised by the Basel Committee (2011). Available at https://www.bis.org/press/p110601.htm
[4] U. Cherubini, Counterparty Risk in Derivatives and Collateral Policies The Replicating Portfolio Approach (2005).
[5] J. Gregory, Being two-faced over counterparty credit risk, Risk (2009).
[6] M. Pykhtin, S. Zhu, A guide to modeling counterparty credit risk, GARP Risk Review July/August (37) (2007) 16–22.
[7] C. Oosterlee, L. Grzelak, Mathematical Modeling and Computation in Finance, first, World Scientific, 2019. ISBN 978-1-78634-794-7
[8] D. Brigo, A. Capponi, Bilateral counterparty risk valuation with stochastic dynamical models and application to credit default swaps, arXiv Electronic Journal (2009).
[9] D. Brigo, M. Masetti, Risk Neutral Pricing of Counterparty Risk (2005).
[10] D. Brigo, A. Pallavicini, V. Papatheodorou, Arbitrage-free valuation of bilateral counterparty risk for interest-rate products: impact of volatilities and correlations, Mathematical Finance 14 (6) (2011) 773–802.
[11] A. Pallavicini, D. Perini, D. Brigo, Funding valuation adjustment: a consistent framework including CVA, DVA, collateral, netting rules and re-hypothecation, arXiv Electronic Journal (2011).
[12] A. Pallavicini, D. Perini, D. Brigo, Funding, collateral and hedging: uncovering the mechanics and subtleties of funding valuation adjustments, arXiv Electronic Journal (2012).
[13] I. Arregui, B. Salvador, C. Vázquez, PDE Models and numerical methods for total value adjustment in european and american options with counterparty risk, Appl. Math. Comput. 308 (2017) 31–53.
[14] C. Burgard, M. Kjaer, Partial differential equation representations of derivatives with bilateral counterparty risk and funding costs, The Journal of Credit Risk 7 (3) (2011) 1–19.
[15] T. Bielecki, M. Rutkowski, Valuation and hedging of contracts with funding costs and collateralization, SIAM Journal on Financial Mathematics 6 (1) (2015) 594–655.
[16] S. Crepey, Bilateral counterparty risk under funding constraints - Part i: pricing, Mathematical Finance 25 (1) (2015) 1–22.
[17] S. Crepey, Bilateral counterparty risk under funding constraints - Part II: CVA, Mathematical Finance 25 (1) (2015) 23–50.
[18] P. Henry-Labordere, Cutting CVA's complexity, Risk 25 (2012) 67–73.
[19] P. Henry-Labordere, X. Tan, N. Touzi, A numerical algorithm for a class of BSDEs via the branching process, Stoch. Process. Their Appl. 124 (2) (2014) 1112–1140.
[20] D. Duffie, Dynamic Asset Pricing Theory, third, Princeton University Press, 2001. ISBN 978-0-691-09022-1
[21] B. Dupire, Pricing with a smile, Risk 7 (1994) 18–20.
[22] E. Derman, I. Kani, Stochastic implied trees: arbitrage pricing with stochastic term and strike structure of volatility, International Journal of Theoretical and Applied Finance 1 (1998) 61–110.
[23] S. Heston, A closed-Form solution for options with stochastic volatility with applications to bonds and currency options, Review of Financial Studies 6 (2) (1993) 327–343.
[24] P. Hagan, D. Kumar, A. Lesniewski, D. Woodward, Managing smile risk, Wilmott Magazine 3 (2002) 84–108.
[25] A. Lipton, The vol smile problem, Risk 15 (2002) 61–66.
[26] S. Kou, A jump-Diffusion model for option pricing, Manage. Sci. 48 (8) (2002) 10861101.
[27] R. Merton, Option pricing when the underlying stock returns are discontinuous, J. financ. econ. 3 (1–2) (1976) 125144.
[28] C. He, J. Kennedy, T. Coleman, P. Forsyth, Y. Li, K. Vetzal, Calibration and hedging under jump diffusion, Review of Derivatives Research 9 (1) (2006) 1–35.
[29] J. Kennedy, P. Forsyth, K. Vetzal, Dynamic hedging under jump diffusion with transaction costs, Oper. Res. 57 (3) (2009) 541–559.
[30] L. Andersen, V. Piterbarg, Interest Rate Modeling - Volume III: Products and Risk Management, first, Atlantic Financial Press, 2010. ISBN 978-0-98442-212-8
[31] V. Naik, M. Lee, General equilibrium pricing of options on the market portfolio with discontinuous returns, Review of Financial Studies 3 (4) (1990) 493–521.